Statens vegvesen

Norwegian Public Roads Administration

Energy absorption capacity for fibre reinforced sprayed concrete. Effect of friction in round and square panel tests with continuous support (Series 4)

REPORT Technology Department No. 2534

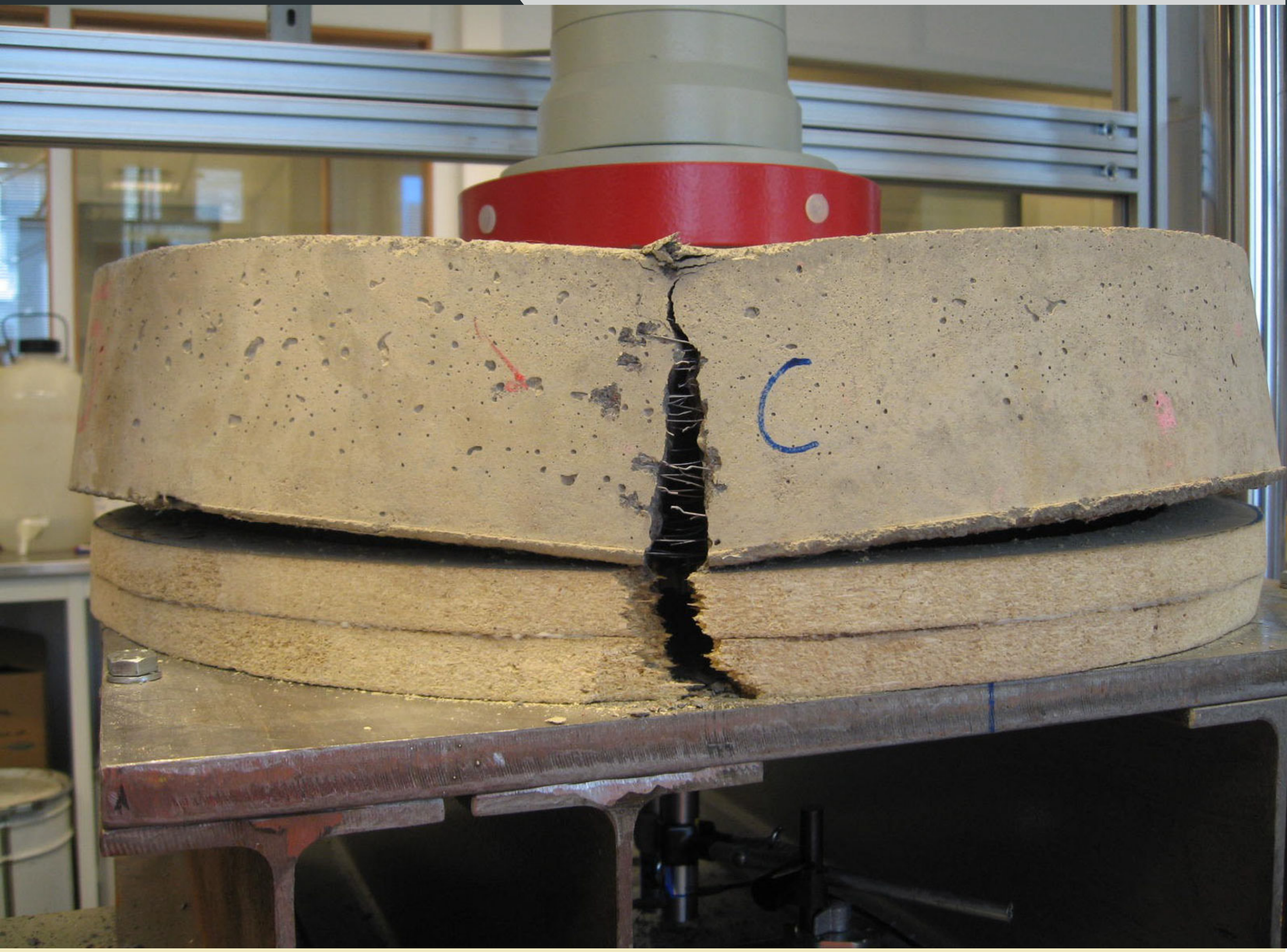

Date: 2009-02-16

Statens vegvesen

Norwegian Public Roads Administration
Directorate of Public Roads
Technology Department

Address: P.O.Box 8142 Dep
N-0033 Oslo

Telephone: +47 915 02030

www.vegvesen.no

TECHNOLOGY REPORT 2534

Title

Energy absorption capacity for fibre reinforced sprayed concrete. Effect of friction in round and square panel tests with continuous support (Series 4)

Authors

Øyvind Bjøntegaard

Date:	Executive officer	Project no.
2009-02-16	Synnøve A. Myren	601420
	Reviewed by	Number of pages
	Synnøve A. Myren	34 / 27

Summary

The present test program is carried out as a part of the on-going revision of the Norwegian Concrete Association's publication no. 7 (Sprayed concrete for rock support), which, among others, is to be harmonized with the new European standards dealing with energy absorption capacity for fibre reinforced sprayed concrete. The new European standards describe square panels (continuous support), while the Norwegian tradition has been to test round panels (also continuous support) as described in the previous version of NB7. The program that has been undertaken is a comparative study of these two methods. The present report gives the results from the fourth test series in this program and is focused on the effect of friction during such tests.

The used concrete mix has a nominal water-to-binder ratio of 0.42 and has a 20 kg/m3 dosage of 35 mm long steel fibres with end-hooks. All specimens were ready-mixed and cast in-situ (not sprayed). The 28-days compressive strength of the concrete was 72 MPa.

The potential effect of friction is the same for round and square panels, presuming that the support material is the same. It is assumed that four perpendicular cracks form and that the cracks are oriented normal to the support. A theoretical evaluation reveals that the effect of friction will be somewhat less for square panels if the cracks are oriented closer to the corners.

The energy absorption capacity (EAC) test results show that the average coefficient of variation (COV) was 7.8 % for the two individual sets with round panels and, similarly, 11.7 % for the square panels. The average COV for EAC for the two different friction conditions were quite similar. The EAC from square and round panels at similar support (friction) conditions corresponded well.

In panel tests with continuous support the friction occurs in two directions; tangential and radial. The tangential- and radial movements of the panel relative to the support have been quantified. The results show that the friction conditions between the concrete panel and the support fixture has a great impact on the measured energy uptake. For the case denoted "standard" conditions, which is the normal set-up for panel tests, the results show that 35% of the overall energy uptake between zero and 25 mm deflection is due to friction, and the remaining 65% is due to fibre action in the concrete panel.

When friction is eliminated in the test, the results show on average, that the maximum load during the test is reduced by 15 % and the residual load at 25 mm deflection is reduced by 46 %.

By using the energy balance equations the coefficient of friction was deduced from the test results. It is found that the coefficient of friction is substantial and that it increases as the test proceeds. This may be associated with a gradual penetration of the sharp concrete crack edges into the wooden support.

Adjustments of the early non-linear behaviour of the load deflection curves have been made in accordance to the procedure in ASTM 1550-05. The adjustments had no significant effect on the calculated energy absorption capacity.

Key words

Fibre reinforced sprayed concrete, energy absorption capacity, round and square panel tests, effect of friction

Summary

The present test program is carried out as a part of the on-going revision of the Norwegian Concrete Association's publication no. 7 (NB 7): "Sprayed concrete for rock support", which, among others, is to be harmonized with the new European standards dealing with energy absorption capacity for fibre reinforced sprayed concrete. The new European standards describe square panels (continuous support), while the Norwegian tradition has been to test round panels (also continuous support) as described in the previous version of NB7. The program that has been undertaken is a comparative study of these two methods. The present report gives the results from the fourth test series in this program.

The used concrete mix has a nominal water-to-binder ratio of 0.42 and has a 20 kg/m^3 dosage of 35 mm long steel fibres with end-hooks. All specimens were ready-mixed and cast in-situ (not sprayed). The 28-days compressive strength of the concrete was 72 MPa.

The investigation involves energy absorption tests on 16 panels, of which 8 were round panels (D=600 mm, thickness=100 mm) and 8 were square panels (600 mm, thickness=100 mm). Half of the two types of panels were tested in the usual way (panel placed directly on a wooden support) whereas for the other half special measures were made to eliminate friction between the panel and the support. It is assumed that there was no friction in these latter tests, but it is likely that a small component of friction was yet present. It is therefore possible that the effect of friction which is proven here is slightly underestimated.

The potential effect of friction is the same for round and square panels, presuming that the support material is the same. It is assumed that four perpendicular cracks form and that the cracks are oriented normal to the support. A theoretical evaluation reveals that the effect of friction will be somewhat less for square panels if the cracks are oriented closer to the corners.

The energy absorption capacity (EAC) test results show that the average coefficient of variation (COV) was 7.8 % for the two individual sets of round panels and, similarly, 11.7 % for the square panels. The average COV for EAC for the two different friction conditions were quite similar. The EAC from square and round panels at similar support (friction) conditions corresponded well.

In panel tests with continuous support the friction occurs in two directions; tangential and radial. The tangential- and radial movements of the panel relative to the support have been quantified.

The results show that the friction conditions between the concrete panel and the support fixture has a great impact on the measured energy uptake. For the case denoted "standard" conditions, which is the normal set-up for panel tests, the results show that 35% of the overall energy uptake between zero and 25 mm deflection is due to friction, and the remaining 65% is due to fibre action in the concrete panel.

When friction is eliminated in the test, the results show on average, that the maximum load during the test is reduced by 15 % and the residual load at 25 mm deflection is reduced by 46 %.

By using the energy balance equations the coefficient of friction was deduced from the test results. It is found that the coefficient of friction is substantial and that it increases as the test proceeds. This may be associated with a gradual penetration of the sharp concrete crack edges into the wooden support.

Adjustments of the early non-linear behaviour of the load deflection curves have been made in accordance to the procedure in ASTM 1550-05. The adjustments had no significant effect on the calculated energy absorption capacity.

Sammendrag

Forsøksprogrammet er gjennomført som et ledd i det pågående arbeidet med revisjon av Norsk Betongforenings publikasjon nr. 7 (NB 7) "Sprøytebetong til bergsikring", som bl.a. skal tilpasses de nye europeiske reglene for bestemmelse av energiabsorpsjonskapasitet for fiberarmert sprøytebetong. De utførte forsøkene er en sammenliknende studie av sirkulære og kvadratiske plateprøver. De nye europeiske standardene beskriver kvadratiske plateprøver (kontinuerlig opplegg), mens norsk tradisjon har vært sirkulære plateprøver (også kontinuerlig opplegg). Programmet som er igangsatt er en sammenliknende studie av disse to metodene. Rapporten presenterer programmets fjerde forsøksserie.

Den anvendte betongen har et nominelt vann-bindemiddel-forhold på 0,42 og er tilsatt 20 kg stålfiber (lengde=35 mm og med endekroker) pr m^3 betong. Alle prøvestykkene ble blandet på blanderi og støpt ut tradisjonelt (ikke sprøytet). Betongens 28-døgnsfasthet var 72 MPa.

Forsøksserien omfatter energiabsorpsjonsforsøk på 16 plater, hvor 8 var runde (D=600 mm, tykkelse 100 mm) og 8 var kvadratiske (600 mm, tykkelse 100 mm). Halvparten av hver platetype ble så testet ved normale/standard forhold (platen legges direkte på opplegget av finer), mens for siste halvpart ble det gjort spesielle tiltak for å eliminere friksjonen mellom plate og opplegg. Det antas at det ikke var friksjon i disse siste forsøkene, men det er sannsynlig at en liten friksjonskomponent likevel var til stede. Det er derfor mulig at friksjonseffekten som er funnet kan være noe underestimert.

Den potensielle effekten av friksjon er den samme for runde og kvadratiske plater, forutsatt at opplegget er av samme materiale. Det er forutsatt at det dannes fire rettvinklede flytelinjer og at alle er orientert normalt mot opplegget. En teoretisk vurdering viser at for kvadratiske plater vil effekten av friksjon bli noe mindre hvis flytelinjene orienterer seg mer mot hjørnene.

Resultatene for energiabsorpsjonskapasitet (EAC) viser at gjennomsnittlig variasjonskoeffisient (COV) ble 7.8% for de to individuelle settene med runde plater og tilsvarende 11.7% for de to kvadratiske settene. Gjennomsnittlig COV for EAC for de to friksjonsforholdene er omtrent like. EAC fra runde og kvadratiske plater med samme friksjonsforhold viser god overensstemmelse.

I plateforsøk med kontinuerlig opplegg opptrer friksjonen i to retninger, tangensiell og radiell. Den relative forflytningen av prøveplata over opplegget er kvantifisert for de to retningene.

Resultatene viser at friksjonsforholdene mellom betongplate og opplegg har stor betydning for det målte energiopptaket. Resultatene viser at 35% av målt EAC ved standard prøvningsoppsett skyldes friksjon mellom prøveplata og opplegget. De resterende 65% av energien opptas pga. fibervirkning i betongplata.

Når friksjonen fjernes i forsøket viser resultatene, i gjennomsnitt, at maksimumslasta under forsøket reduseres med 15% og at reststyrken ved 25 mm nedbøyning reduseres med 46%.

Friksjonskoeffisienten for glidningen mellom betongplata og opplegg er dedusert ved bruk at likningen for energibalanse. Friksjonskoeffisienten er betydelig og den øker gradvis under forsøkets gang. Økningen kan skyldes at de skarpe risskantene i betongplata til en viss grad penetrerer opplegget.

Justering av det ikke-lineære kraft-deformasjonsforløpet før opprissing er gjennomført i henhold til prosedyren som er beskrevet i ASTM-standarden (ASTM 1550-05). Justeringen hadde ingen signifikant effekt på beregnet energiabsorpsjonskapasitet.

Content

1 Introduction

The present test program is carried out as a part of the on-going revision of the Norwegian Concrete Association's publication no. 7 (NB 7): "Sprayed concrete for rock support"[1] (in Norwegian: "Sprøytebetong til bergsikring"), which, among others, is to be harmonized with the new European standards dealing with energy absorption capacity for fibre reinforced sprayed concrete. The new European standards describe square panels (continuous support), while the Norwegian tradition has been to test round panels (also continuous support) as described in the previous version of NB7. The program that has been undertaken is a comparative study of these two methods.

During quality control the test panels shall, according to the standards, be sampled with the relevant concrete, personnel and spraying equipment (robot) for the given project. Some 10 years ago in Norway, it was decided to use round panels (600 mm diameter, 100 mm thick, net weight around 65 kg). These panels can be produced where the actual spraying work is done and they are experienced to be quite easy to sample and subsequently to be removed by two persons to a safer place in the tunnel.

According to the new European regulations (EN 14488 part 1 and part 5, [2][3]) large 1000 mm x 1000 mm (100 mm thick) panels shall be sprayed (net weight around 230 kg) and the panels shall not be removed the first 18 hours. After that, all further handling must be machine-based. Later in the laboratory, the panels shall be saw-cut in to a final size of 600 mm x 600 mm (net weight about 83 kg). By this rigorous procedure we fear that the connection between testing and practical application may be lost. It is also a big challenge to trim a 1000 x 1000 mm panel within the given tolerances for thickness.

The scope of the project as a whole is to study the practical consequences of the new regulations and to carry out comparative tests on energy absorption capacity on round and square panel tests.

Cooperation is established with the contractor Entrepenørservice with regard to building of moulds and production of test panels. Members of the Norwegian Concrete Association's Sprayed Concrete Committee also contribute. The tests are performed in the Norwegian Public Roads' Central laboratory.

Up till now (2007-2008) four test series have been carried through, all with field-produced round- and square panels. The present report gives the results from Series 4. The results from Series 1-3 are reported separately. [7]-[9]

2 Friction; background and theory

The scope of the present investigation was to study the effect of friction during energy absorption capacity tests on round and square panels with continuous support. The motive for studying the effect of friction was some direct observations of friction that was done during the second series in our test program (Series 2, reported in [8]). In addition to this, a 15-20% effect of friction has been reported for the ASTM-panels [10] (having 3-point determinate support conditions). Any friction forces between the concrete panel and the support fixture during testing, independent of type of support, will be taken as inner work and erroneously be calculated as energy uptake of the concrete. Hence, during a test the work from friction will be taken to be inner work exerted by the panel and, thus, the measured energy absorption capacity will be overestimated.

During the previous Series 2 failure of the support ring was observed, see Fig. 2.1. The failure must be due to tangential friction. This friction work to hinder the opening of the crack transferring tensile stresses to the support and, in this case, causing tensile failure of the support.

Since the central part of the panel is pushed downwards by the central load the only contact zone between the support and the panel will then be at the inner side of the support. In the post-cracking period all transmission of load will then take place over the sharp crack edge zones and the inner side of the support, thus the counterforce from the support will occur as point loads. Consequently, the point-loads (the local stress) in these contact zones will be high. This is illustrated in Fig. 2.2. Each crack naturally consists of two crack edges, and for four perpendicular cracks in the panel the load at each contact-point with the support then will be P/8. For an external load of for instance P=50 kN this means that a vertical load of P/8=6.25 kN (~ 640 kg) is transferred over each contact-point.

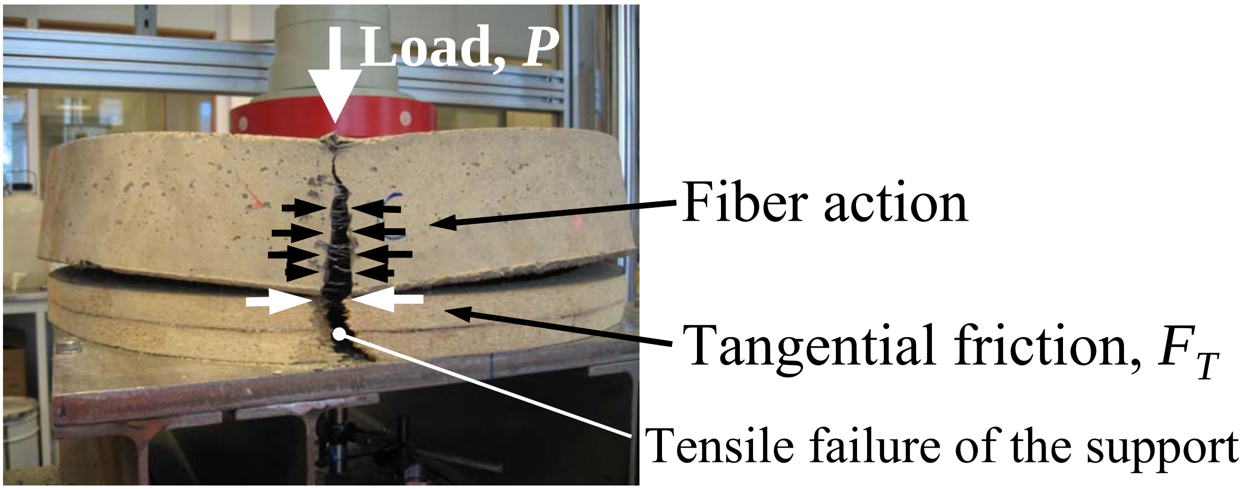

Fig. 2.1 Tensile failure of the support caused by tangential friction. Previous test, Series 2 [8].

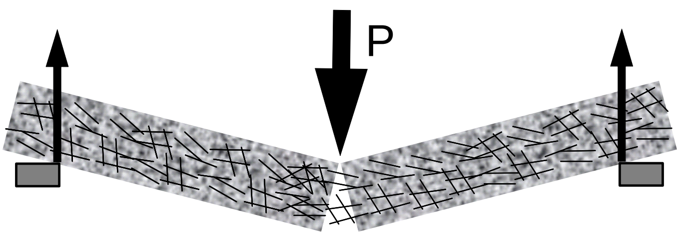

Fig. 2.2 Illustration of loading and rotation of the panel causing point-loads at the inner side of the support.

The friction force (F) is given by the coefficient of friction (μ) and the normal force (P) as follows:

Equation 1 $$F = \mu P$$

The contribution from friction (W_F) in the energy balance will then be the integral of the friction force (F) multiplied with the movement of the panel (w_F) over the contact zone with the support. In our case w_F will consist of a tangential, w_T, (as shown in Fig. 2.1) and a radial, w_R, component. As the panel is pushed down and rotated, the crack edges slide tangentially as well as radially because the under-side of the panel is pushed outwards. The radial movement is indicated in Fig. 2.3, showing a cross-section of half a panel. As shown, it is assumed that the crack opens over the whole height of the panel and there is only contact at the top, which should be quite accurate since the compressive zone at the top is generally quite small after cracking. For incremental total movement dw_F of the panel in the contact zone with the support the total energy from friction W_F then be expressed as:

Equation 2 $$W_F = \int F dw_F = \int \mu P dw_F$$

Tangential- and radial movement for one crack is shown in Fig. 2.4. The total picture of potential friction forces working on round and square panels is shown in Fig. 2.5.

The standards describe that the energy absorption capacity (EAC) from a test is to be calculated as the external work from the load P (W_P) under the assumption that it equals to the inner work by the panel ($EAC_{standard} = W_p = W_i$). However, considering the above discussion the contribution from friction energy (W_F) should be taken into consideration and from a fundamental standpoint the following relation is then the valid one:

Equation 3 $$W_P = W_i + W_F \qquad \text{hence} \qquad W_i = W_p - W_F = \int P d\Delta - \int \mu P dw_F$$

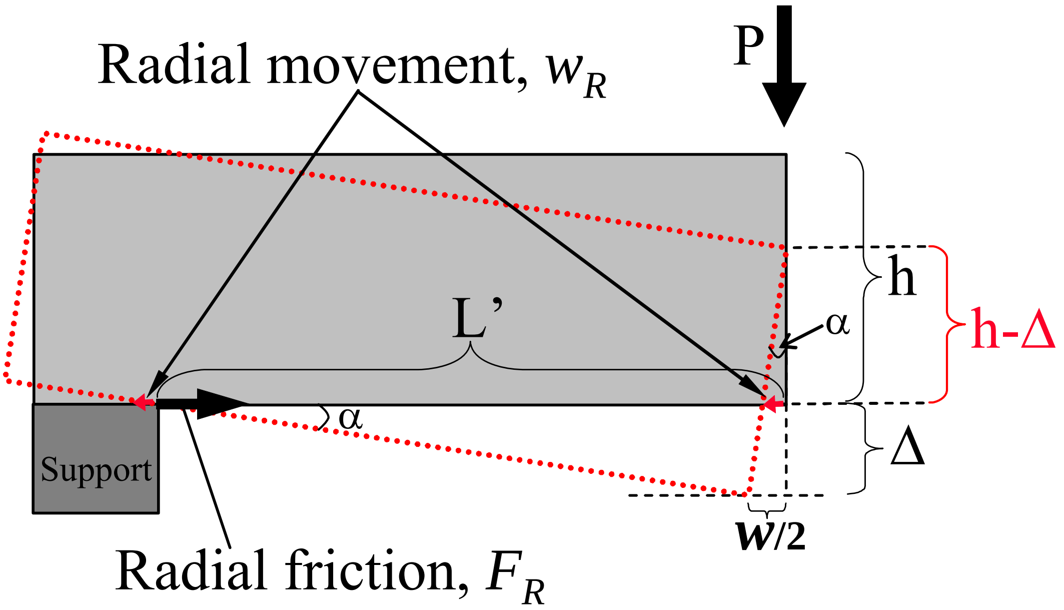

Fig. 2.3 Radial movement and friction at the underside of the panel during testing. Cross section of half the panel.

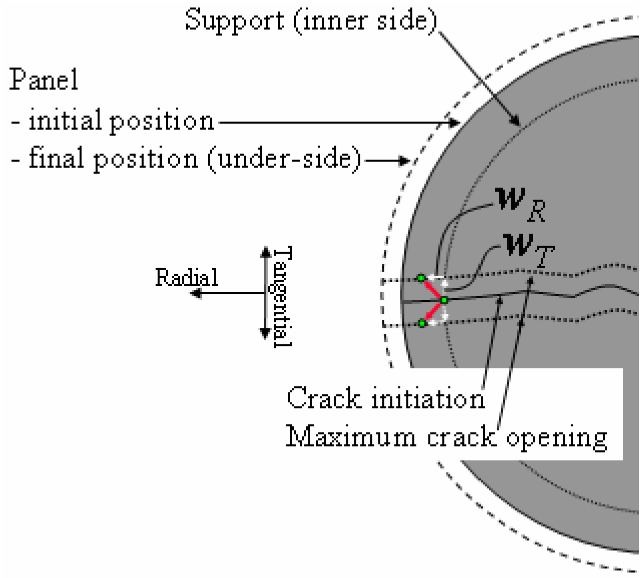

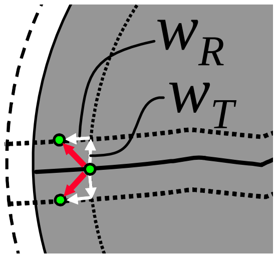

Fig. 2.4 Sliding of the two crack edges, from initial cracking (middle green dot), and then in tangential and radial direction. The red arrows illustrate the resulting movement of the crack edges during the final opening of the crack.

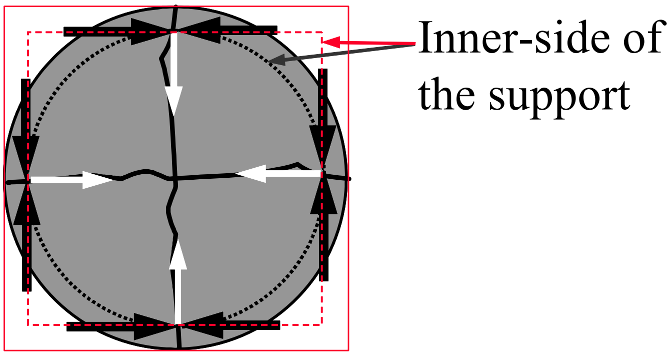

Fig. 2.5 Potential tangential- (black arrows) and radial (white arrows) friction forces in round and square panels with continuous support. Assumption: Four perpendicular cracks meeting the support with an angle of 90°.

Consequently, since EAC from standard set-up ($EAC_{standard}$) equals W_P there will be an error if friction is present (i.e. when $\mu > 0$). When friction is present the correlation between the actual inner work W_i of the panel and $EAC_{standard}$ is really:

Equation 4 $$W_i = EAC_{standard} - W_F$$

The following theoretical evaluation is made to enhance the understanding of the behaviour of the panels during testing as well as to enable a calculation of the effect of friction (see Chapter 8). The evaluation assumes that four perpendicular cracks occur during the test (in both round and square panels, as shown in Fig. 2.5) and that there is no bending of the concrete between the cracks, hence all deformation occurs in the cracks. The pre-cracking period (lasts from zero up to some millimetres deflection) is overlooked despite the fact that the present experimental results reveal that friction appears to play a significant role also in this period, which is seen as the maximum load being clearly affected by friction (see Section 6.7). As the panel is pushed downward, the pre-cracking period will be associated with elastic bending and inward radial movement of the panel relative to the support; a movement which naturally may be associated with friction. At the point of cracking the elastic deformation is released as cracks causing an abrupt outward radial movement, as well as tangential movement. The further pre-cracking behaviour is discussed below. The pre-cracking period constitute the majority of the deflection range and by far the majority of the energy uptake during the test.

As long as four perpendicular cracks meet the support with an angle of 90° the friction condition is similar for round and square panels. For the square panels the situation change a bit if the four cracks are oriented more towards the corners. This situation is discussed briefly at the end of this section.

To simplify the evaluation, it is assumed in the following that $\sin\alpha = \tan\alpha = \alpha$ for small angles. For central panel deflections from zero to 25 mm the error of this simplification is not larger than 1-2%. Assuming the four perpendicular cracks the rotation (α) of the panel will be:

Equation 5 $$\tan\alpha = \frac{\Delta}{L'}$$

where *L'* is the free span from the inner edge of the support to the center (250 mm) and *h* is the thickness of the panel (100 mm), see Fig. 2.3.

The movement of one contact-point of the crack relative to the support in the <u>tangential direction</u> (w_T) equals to half of the crack opening, *w/2*, hence:

Equation 6 $$w_T = \frac{w}{2} = \tan\alpha \cdot h = \frac{\Delta \cdot h}{L'}$$

At maximum central displacement (Δ_{max}=25 mm) $w_{T,max}$ then becomes 10 mm.

A simplified geometrical consideration gives the following relation between the <u>outward radial movement</u> (w_R) and *w/2*:

Equation 7 $$\frac{w_R}{w/2} = \frac{(h-\Delta)\tan\alpha}{h \cdot \tan\alpha} = \left(1 - \frac{\Delta}{h}\right) \qquad \text{hence} \quad w_R = \frac{1}{2}\left(1 - \frac{\Delta}{h}\right)w$$

The displacement Δ and crack opening *w* are interrelated, and during increasing displacement (increasing *w*) the radial movement w_R will decrease linearly compared to *w*. The total radial movement w_R from Δ=0 to a specified deflection Δ_γ then can be expressed as:

Equation 8 $$w_R = \frac{1}{2}\int_{\Delta=0}^{\Delta_\gamma}\left(1 - \frac{\Delta}{h}\right)dw$$

And, when combining with Equation 6 we get:

Equation 9
$$w_R = \frac{h}{L'} \int_{\Delta=0}^{\Delta_\gamma} \left(1 - \frac{\Delta}{h}\right) d\Delta$$

After performing the integral w_R then becomes:

Equation 10
$$w_R = \frac{h}{L'} \left[\Delta - \frac{\Delta^2}{2h} \right]_{\Delta=0}^{\Delta_\gamma}$$

Finally, at each contact-point with the support there will be a relative movement/sliding governed by the tangential- and radial component given by Equation 6 and Equation 10, respectively. The two components are perpendicular to each other, hence the total resulting movement/sliding (w_F) along the support from Δ=0 to Δ_γ then can be found by the use of Pythagoras:

Equation 11
$$w_F = \sqrt{w_T^2 + w_R^2} = \sqrt{\left(\frac{\Delta_\gamma \cdot h}{L'}\right)^2 + \left(\frac{h}{L'}\left[\Delta_\gamma - \frac{\Delta_\gamma^{\ 2}}{2h}\right]\right)^2}$$

It follows then that for the whole test range (Δ_γ = 25 mm) that w_T is 10 mm and w_R is 8.75 mm, and the total sliding along the support w_F becomes 13.3 mm. The energy from friction during an energy absorption capacity test can now be determined numerically by combining Equation 2 and Equation 11, giving Equation 12.

Equation 12
$$W_F = \sum_{\Delta=0}^{\Delta_\gamma} \mu_\Delta P_\Delta dw_F = \left[\mu_\Delta P_\Delta \sqrt{\left(\frac{\Delta_\gamma \cdot h}{L'}\right)^2 + \left(\frac{h}{L'}\left[\Delta_\gamma - \frac{\Delta_\gamma^{\ 2}}{2h}\right]\right)^2} \right]_{\Delta=0}^{\Delta_\gamma}$$

In Chapter 8 this equation is applied on the experimental results. As already mentioned, in a square panel an orientation of the (four) cracks more towards the corners will theoretically affect the movement of the panel relative to the support. As the cracks orientate closer to the corners, the free span between the inner side of the support and the center of the panel (*L'*) will increase and the rotation of the panel will therefore be less. Assuming that the cracks go through the corners *L'* will be maximum, and it will then be $\sqrt{2}$ times the *L'* (=250 mm) discussed earlier. Consequently, w_T, w_R and w_F then become $1/\sqrt{2}$ (=0.71) times the values above, hence w_F will be 13.3 mm x 0.71 = 9.4 mm. This means that for “corner-cracks” in a square panel the effect of friction is theoretically 71 % of that when cracks are oriented perpendicular to the support.

3 Test program

The investigation is based on one specific basic sprayed concrete composition. All specimens were cast, not sprayed, hence accelerator was not used. The following measurements were performed:

- Slump (visually) and air content: Performed at the casting site
- Fibre content in fresh concrete: Fresh concrete was transported to the laboratory where the measurements were performed
- Compressive strength on two 100 x 100 mm cubes after 7 days and two cubes after 28 days

- Energy absorption capacity of 8 round panels (Ø600 mm, thickness=100 mm) and 8 square panels (sides=600 mm, thickness=100 mm) were tested according to the procedures in respectively NB 7 (round) and EN 14488-5 (square), with the exception for the square panels that the support-frame was made of the similar wooden material as for the round panels, and not steel as described in EN 14488-5:

    - Half of the round and half of square panels were tested according to standard procedure, meaning that the panels were placed directly on the support. **This set-up is denoted "Standard" (std) conditions**

    - For the second half of round and square panels it was taken measures to eliminate the friction between the specimen and the support fixture. **This set-up is denoted "No friction" (no fr.) conditions**

Due to an error in the control and logging system which occurred after the first set of panels, and a successive period with repair, the panels were tested at somewhat different concrete ages. This is believed not to have affected the findings in the report to a significant degree. The issue is dealt with in Section 6.6. The test ages for the panels became:

Square panels, "standard" conditions: Concrete age = 40 days
Round panels, "standard" conditions: Concrete age = 60 days

Square panels, "no friction" conditions: Concrete age = 61 days
Round panels, "no friction" conditions: Concrete age = 61 days

4 Concrete mix, casting and curing

4.1 Concrete mix

The mixing of the concrete was done 4th of April 2008 at the ready-mix plant of Unicon in Oslo (Sjursøya). The concrete was then transported by concrete lorry about 30 min to a nearby construction area (Vinterbro), where all casting took place in a tent.

The nominal recipe of the basic sprayed concrete mix (Table 1) is quite the same as that of the previous investigations [7], [8], [9]. The concrete was cast, hence no accelerator was added. The nominal (effective) water-to-cement ratio (w/(c+2s)) is 0.42. The nominal fibre dosage is 20 kg/m^3. The fibre is 35 mm long, 0.54 mm thick and has end-hooks. Concrete mixing log and data sheet for the fiber is given in APPENDIX 1 and APPENDIX 2, respectively.

Table 1: Nominal concrete mix

Material	Type/producer	Kilo pr. m^3 concrete
Cement (1)	Norcem Standard FA Cem II/A-V 42.5R	226
Cement (2)	Norcem Anlegg CEM I 52,5N	225
Silica fume(k=2)	Elkem microsilica	22
Sand, 0-8 mm	Svelviksand	1572
Steel fibre	Dramix 65/35 / Bekaert	20
Superplasticizer	Glenium Sky 552 / BASF	4,1
Retarder	Delvocrete stabilisator / BASF	1,49
Air entraining	Micro air (1:19) / BASF	0,94
Pump enhancer	TCC 735 N	
Free water		208
Nominal density		2275

4.2 Casting and curing of panels

16 panels were cast in total; 8 round and 8 square panels. Both types of panels have a nominal thickness of 100 mm. The moulds for the round panels were made of steel all through (Ø600 mm inner diameter) whereas the moulds for the square panels were made of 22 mm plywood (100 mm high and with 600 x 600 mm inner dimensions) nailed down to a pallet, hence all panels were cast into their final size.

Square and round panels were cast every second time and numbered successively:
The square panels were numbered 1, 3, 5, 7, 9, 11, 13 and 15
The round panels were numbered 2, 4, 6, 8, 10, 12, 14, 16

After casting the panels were covered with plastic foil. De-moulding took place 4 days after casting. All specimens were then transported to the Central laboratory of the Norwegian Public Roads Administration (NPRA) where they were stored in water until the day of testing.

5 Test methods and -procedures

5.1 Air content

Air content was measured in fresh concrete, standard method. [4]

5.2 Fibre content

Two samples, each consisting of 1 litre concrete, were tested. The weight of the sample was measured. The concrete from the sample was then washed, in portions, over a 1 mm sieve and the fibres were taken out by an electron magnet and washed completely clean afterwards. When the fibres were completely dry, after a period with air drying (a couple of hours), the total weight of fibres in each sample were determined and the ratio fibre content (gram) to concrete volume (1 litre) was found. The procedure is in accordance with EN 14488-7:2006 [5].

5.3 Compressive strength

100 x 100 mm cubes were tested according to standard procedure (load rate = 0.8 ± 0.2 MPa/sec). [4]

5.4 Energy absorption capacity

5.4.1 Test rig

The set-up for the round and square panels is shown in Fig. 5.1. Note that the support fixtures for both panel types were the same (plywood of birch). The plywood support is 40 mm high and 50 mm wide and has an inner diameter/length (round/square) of 500 mm. According to EN 14488-5 the square panels shall be put on a support fixture of steel with bedding material in between (mortar or plaster), whereas NB 7 describes plywood without bedding material. However, in order to ensure a direct comparison of both the friction effect and the panel type identical support conditions was chosen, i.e. support of plywood and no bedding material.

The central displacement of the panels was measured by two transducers as shown in Fig. 5.2. The transducers are spring-loaded, and they are of the type "ACT1000A LVDT Displacement Transducer" from RDP Group. The measuring range is 50 mm.

A steel plate was put between the central oriented load cell and the specimens, a Ø100 mm cylindrical plate for the round panels (+ a thin sheet of cardboard) and a 100 x 100 mm square plate (+ a thin sheet of cardboard) for the square panels.

The test machine (FORM+TEST Delta 5-200 with control system Prüfsysteme Digimaxx C-20) has a maximum load of 200 kN. The deformation rate during the test is controlled by the average signal from the two displacement transducers. Prior to the test, the load-cell is stabilized at a load of 1 kN. With this initial load the test is started.

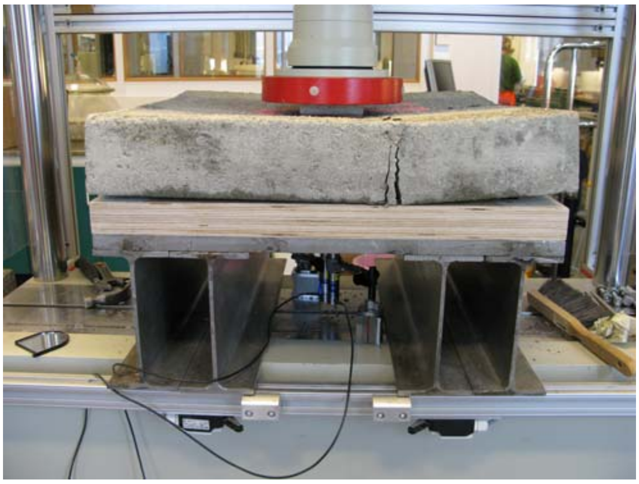

Fig. 5.1 Set-up for energy absorption tests on round (left) and square (right) panels. For both types the support fixture was made of plywood of birch.

Fig. 5.2 Measurement of central displacement at the bottom side of the panel by the use of two spring loaded displacement transducers (LVDT) with discs on top which can rotate along with the rotation of the panel, as well as bridging over the cracks.

5.4.2 Test procedure

Prior to testing, each panel was taken out of the water bath and transported to the test rig. The test started within 45 minutes.

The procedure was then as follows:

1) The mid-point was marked on the smooth moulded face of the panel.
2) The panel (both square and round) was then placed in the test rig with the <u>smooth moulded face against the support fixture</u>, and centered. For the panels tested under "standard" conditions there was direct contact between the concrete specimen and the support, while for

the panels tested under “no friction” conditions two layers of plastic sheets with grease in between was placed between specimen and the support, see next section.

3) Two displacement transducers were placed under the center of the panels. The average of the two transducers forms the signal for load control.
4) On the upper side of the panel (the cast side) a load plate was placed at the center (+ a thin sheet of cardboard).
5) The load cell is prepared for testing by lowering it to the load plate until a load of 1 kN is applied to the panel.
6) The test is then started and load and deflection signals are logged continuously by a computer. According to NB 7 the load was applied deformation-controlled at a rate of 1.5 mm/min central deflection for the Round panels, and according to EN 14488-5 at a rate of 1.0 mm/min central deflection for the Square panels. (based on other results [6] it is no reason to believe that this (small) difference in load-rate has any influence on the result)
7) The test was stopped automatically when the central deflection was 30 mm.
8) The panel was then lifted out of the test rig, the bottom side of the panel was photographed. It was then completely broken into pieces along the cracks and over each cracked surface 3-4 thickness measurements were made. The thickness was measured with a digital sliding calliper.
9) The energy absorption capacity was then calculated as described in the standards (Chapter 6), hence as the area under the load-deflection curve from zero to 25 mm deflection. The results are corrected for thickness when deviating from 100 mm, see Section 5.4.4.
10) In addition the energy absorption capacity was also calculated after correcting the load-deflection curves for the non-linear behaviour during the early loading phase (Chapter 7).

5.4.3 “Standard”- and “no friction” conditions

Half of the concrete panels (4 square and 4 round) were tested under <u>standard conditions</u>. This means that the panels were placed directly on the wooden support frame, see Fig. 5.3.

For the second half of the concrete panels measures were taken to <u>eliminate friction (no friction conditions)</u>. The actions to obtain little/no friction were the following: two layers of 1.5 mm thick strips of plastic sheet with grease in between were put on top of the support frame, see Fig. 5.4 and Fig. 5.5. The strips were about 10 mm wider than the width of the support frame (which is 50 mm wide). The plastic sheets were considered strong and robust, and able to avoid penetration of the sharp edges of the cracks into the support. They also limit stress concentrations under each crack. About ¾ of the width of the upper plastic strip was cut (from inside and outwards) to eliminate the overall axial elasticity of the plastic layer.

After placing the panels on the support frame with the two layers of plastic sheets (and grease in between) it was observed that the friction (in uncracked state) was very low. The heavy panels could be moved quite easily by pushing them sideways with one finger. Product data sheets for the plastic layers are given in APPENDIX 3.

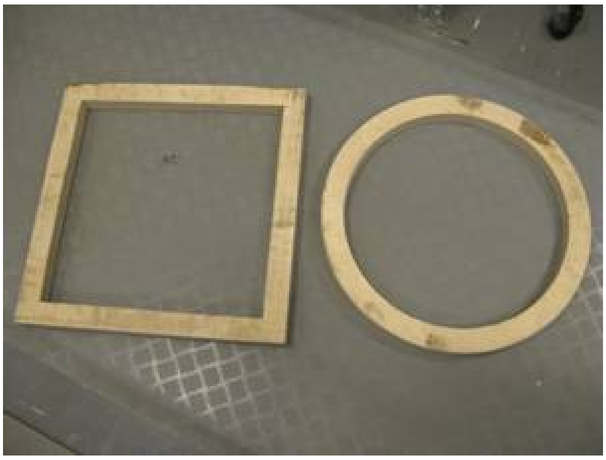

Fig. 5.3 Support frame, "standard" conditions

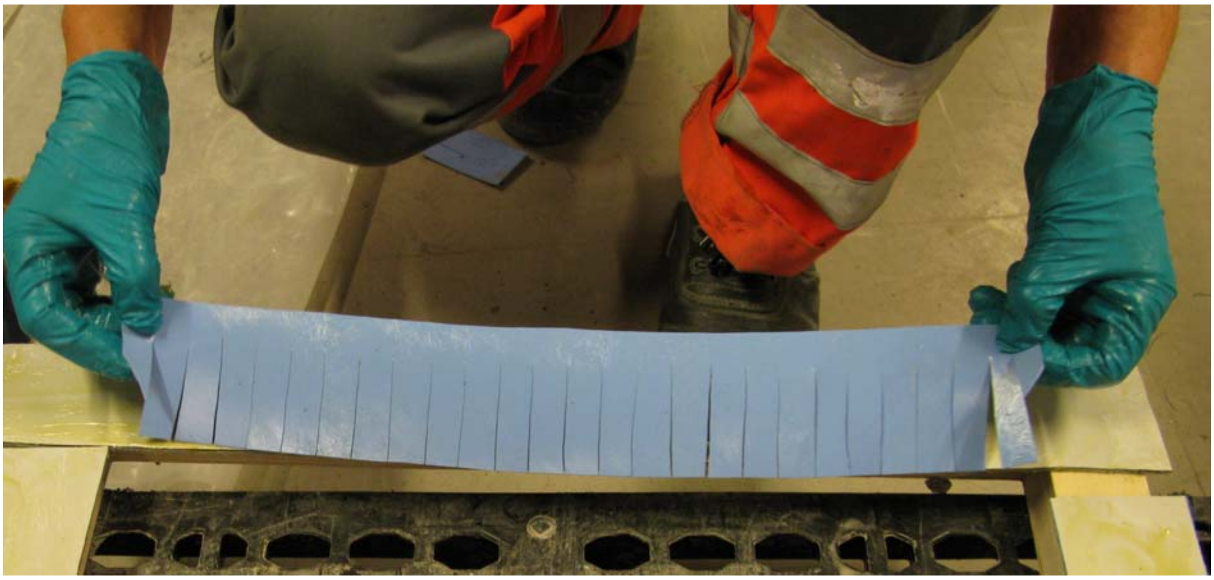

Fig. 5.4 Preparing the support frame for "no friction" conditions. Two layers of plastic sheet with grease in between were put on top of the frame. The upper sheet was cut about ¾ of the width from the inside and outwards.

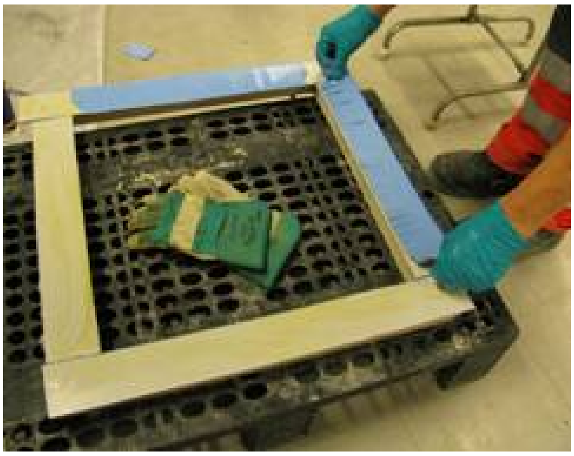

Fig. 5.5 Preparing the support frame for "no friction" conditions. The plastic sheet layers (with grease in between) were put on top of the support frames to completely cover the whole top area plus about 10 mm extra at the inner side of the support.

5.4.4 *Evaluation of results / correcting for deviating thickness*

The energy absorption capacity of the panel shall according to the standards be calculated as the energy uptake between 0 and 25 mm central deflection during a fixed deflection rate. The panel thickness influences the ability to take up energy, where increased panel thickness will increase the energy uptake, and vice versa. Consequently, the calculation of energy absorption capacity should be corrected for this when the thickness is deviating from the reference thickness. A theoretical evaluation of the effect of panel thickness was done in [11]. Target panel thickness is in our case h_0 = 100 mm. The following analysing procedure was proposed for panels with thickness h deviating from h_0:

1. Accumulated energy should be calculated under the load-displacement curve between 0 and a modified displacement $\Delta_m = 25$ mm $\cdot$ k, and $k = 100/h$
2. Calculated EAC should then be multiplied with the factor k.
3. The final corrected EAC is then the result from the test.

The procedure assumes that four cracks develop and that the moment intensity in the crack is given by the crack angle. The total moment capacity is then linearly related to the thickness of the panel and the crack opening. It is likely that the correcting procedure will be valid within reasonable variations in panel thickness and that it will certainly contribute to achieving more comparable results.

What the procedure does is really to normalize the cross section of the yield lines, in horizontal direction by point (1) and in vertical direction by point (2). The following formula is then used to calculate the corrected energy absorption capacity (EAC) in each test:

Equation 13

$$EAC = k \sum_{i=0}^{i=\Delta_m} \left[\left(\Delta_{i+1} - \Delta_i\right) \frac{P_i + P_{i+1}}{2} \right]$$

where k and Δ_m are explained above. Δ is the central displacement, P is the central load and the parameter i is the increment number.

All presented results are corrected according to the above procedure. In the present investigation the panels had thicknesses ranging from 101 mm to almost 107 mm. For the 101 mm panel (“R6”) the correction for thickness reduces the energy absorption capacity by 1.5 % compared to the uncorrected (measured) capacity. Similarly, for the almost 107 mm thick panel (“R12”) the correction was 10%.

6 Results and discussion

6.1 Slump and air content

Slump was not measured, but was visually considered to be around 200 mm. The air content was measured once, showing 3.0 % air.

6.2 Density and fibre content

The measurements on the two fresh concrete samples gave a density of 2282 and 2274 kg/m^3 (average=2278 kg/m^3) and a fibre content of 21.8 and 19.7 kg fibre/m^3 concrete (average=20.8 kg fibre/m^3 concrete), hence the measured density and fibre content corresponds well with the nominal values.

6.3 Compressive strength

The four 100x100 mm cubes were tested at 7 and 28 days concrete age. The results are given below.

Table 2 Compressive cube strength (MPa) after 7 and 28 days concrete age

	7 days	28 days
Cube 1	49.8	69.4
Cube 2	51.2	73.8
Average	50.5	71.6

6.4 Crack pattern

After end of testing, the panels were taken out of the test frame and the bottom side of the panels were then photographed. The pictures are shown in the following two figures. The panels that were tested at “standard” conditions developed 4-5 cracks, while those tested at “no friction” conditions developed 4 cracks.

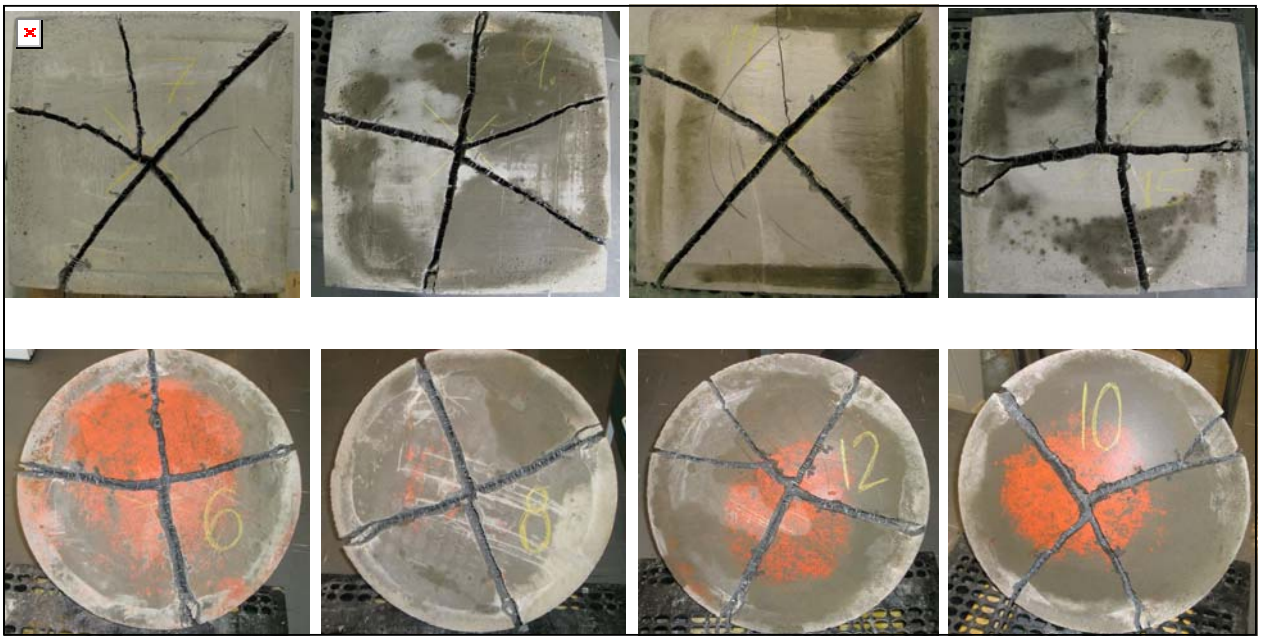

Fig. 6.1 Crack pattern, “standard” conditions

Fig. 6.2 Crack pattern, “no friction” conditions. Square panel no. 3 (“S3”) was not photographed.

6.5 Panel thickness

Measured average panel thicknesses (and standard deviation) are given the previous section. All single measurements are given in APPENDIX 4. The average panel thickness was within the range 101 to 105 mm except for panel “12” being 106.6 mm. The panel thickness is corrected for when calculating the energy absorption capacity according to the procedure described in Section 5.4.4.

Table 3 Average panel thickness and standard deviation

Standard conditions

	Square				Round			
Panel no.	15	9	7	11	6	8	12	10
Average thickness	101.5	102.1	103.5	102.3	101.0	104.2	106.6	102.5
Std.deviation	0.4	1.4	1.2	1.2	1.4	2.4	2.0	1.4

No friction conditions

	Square				Round			
Panel no.	3	1	13	5	16	2	4	14
Average thickness	102.4	102.9	102.4	103.0	101.3	102.7	101.0	103.0
Std.deviation	0.7	0.6	0.6	0.8	0.5	1.2	1.0	0.4

6.6 Energy absorption capacity (EAC); normal analyzing procedure

6.6.1 Variability

The coefficient of variation (COV) among the four sets of panels is shown in Fig. 6.3. Each set consist of four panels. The average COV for all individual sets is 9.7 %.

For the two individual sets of square panels (S) the average COV is 11.7%, and for the two sets of round panels (R) 7.8%. For the two individual sets tested at “standard” conditions (“S(std)” and “R(std)”) the average COV is 10.1%, and for the two sets tested at “no friction” conditions (“S(no fr.)” and “R(no fr.)”) the average COV is 9.4%.

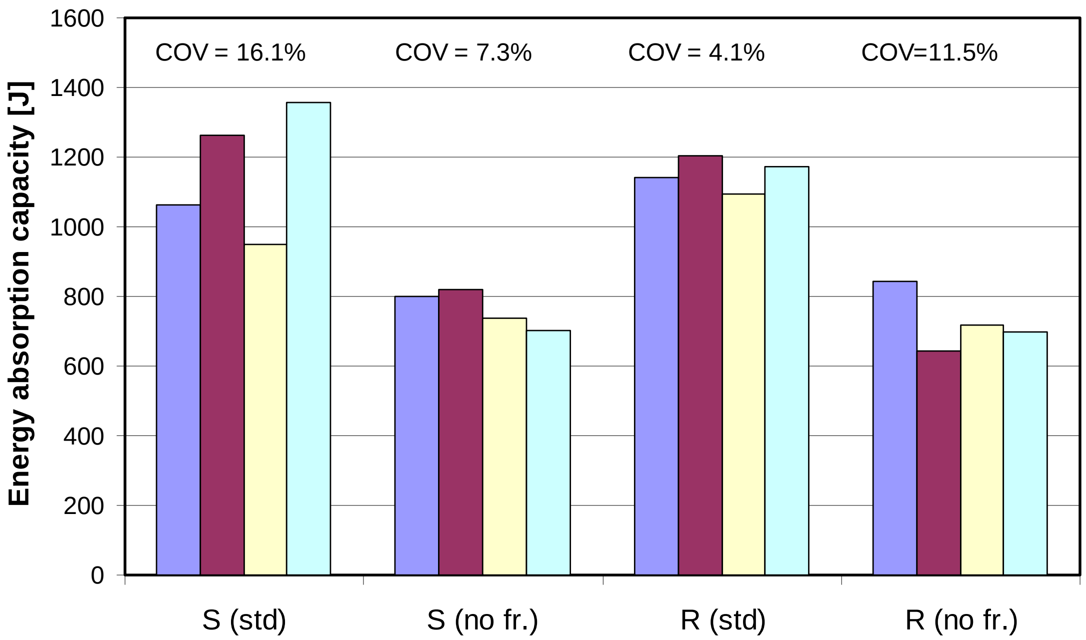

Fig. 6.3 Single results and variability (COV) in each set of panels. (S=square panels, R=Round panels, std=standard conditions, no fr.=no friction conditions)

6.6.2 Effect of friction

The average result for each of the four sets is shown in Fig. 6.4 whereas measured load-displacement for each single test is shown in Fig. 6.5 and Fig. 6.6. It is quite clear that the elimination/reduction of friction had a great impact on the results:

Average energy absorption capacity for all panels with “standard” conditions is 1155 J.
Average energy absorption capacity for all panels with “no friction” conditions is 745 J.
On average the relation “no friction”/“standard” conditions is then 745/1155 = 0.65

As mentioned earlier in Chapter 3 the age at testing differed among the panels due to some error in the logging system. The Square panels tested at “standard” conditions are the deviating ones with 40 days testing age whereas the rest of the panels were 60 and 61 days old when tested. The development of energy absorption capacity from 40 to 60 days is not known, but according to the literature, for instance [14], it could be either a slight increase or a slight decrease, or no change at all. Consequently, it is reason to believe that the given test ages have not influenced any of the main findings and conclusions in the report.

The energy absorption capacity (EAC) results above then reveal that for panels with standard support conditions ($EAC_{standard}$) only 65% of the measured energy is due to fibre action, whereas 35% energy comes from friction, hence:

Equation 14 $$W_i = 0.65 \cdot EAC_{standard} \quad \text{and} \quad W_F = 0.35 \cdot EAC_{standard}$$

where W_i is inner work from the panel (fibre action) and W_F is external work from friction.

The 35 % effect of friction found here is then clearly higher than the 15-20 % effect that is found for the ASTM-panels with 3-point support [10]. The ASTM set-up is associated with radial friction, whereas the present tests (continuous support) are associated with both tangential- and radial friction, as well as point-loads at the contact zones with the support, which supposedly can cause a penetration of the crack edge into the support.

Note that the early load-displacements curves for the “no friction” panels clearly show a non-linear behaviour, see close-up in Fig. 6.7. A significant part of this non-linearity is probably due to squeezing of the two layers of plastic sheets during loading. The panels tested at “standard” conditions have no plastic sheets installed, but still there is some tendency of early non-linearity, which has also been seen during all previous testing. Correcting for the non-linearity (for all panels) has however no significant effect on the results, this is discussed in Chapter 7.

Rapid drops in the load during testing are likely to indicate that cracks are formed, but from the load-deflection records (see for instance Fig. 6.7) it is notable that there are drops in the load up to deflection levels beyond what would be expected from crack formation. This is most pronounced for the “standard” condition tests. For these tests there is also a clear tendency of strain-hardening behaviour, which is quite surprising for the given low steel fibre content of 20 kg. One possible explanation to this behaviour could be that the friction changes between kinetic friction (associated with a high coefficient of friction, i.e. it periodically obstructs the opening of the cracks), and dynamic/sliding friction (having a lower coefficient of friction). If this is the case the friction could in principle produce local load-maximum where dynamic friction suddenly occurs after a period with kinetic friction. The issue is also further discussed in Section 6.7.

The tendency of strain-hardening behaviour is also seen in the previous tests on concretes with similar low fibre content, and with “standard” test conditions.

According to the present results, as expressed in Equation 14, the consequence of the findings is that if a fibre reinforced concrete panel is to have an energy absorption capacity of for example 700 J purely due to fibre action, the measured energy from a test with standard conditions should then be minimum 700 J/0.65 = 1077 J.

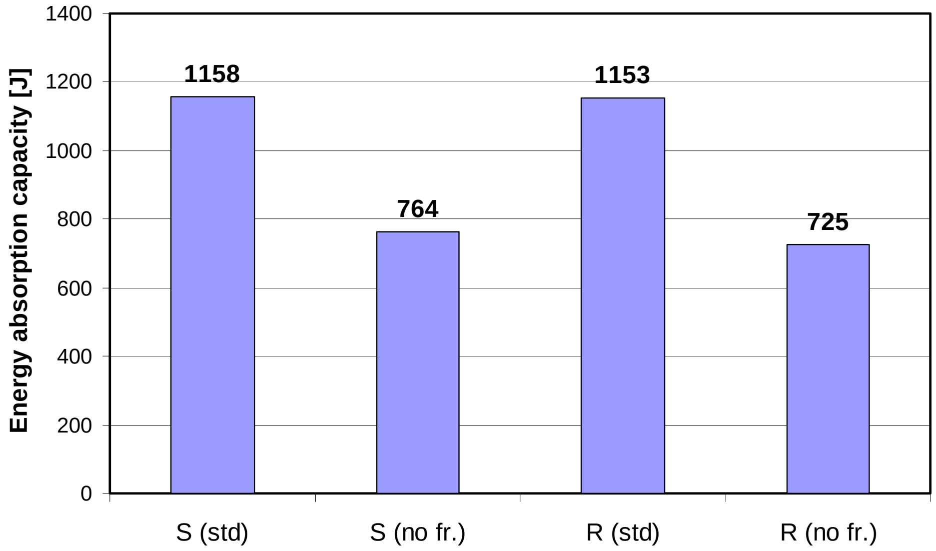

Fig. 6.4 Average energy absorption capacity in each set, corrected for panel thickness. (S=square panels, R=Round panels, std=standard conditions, no fr.=no friction conditions)

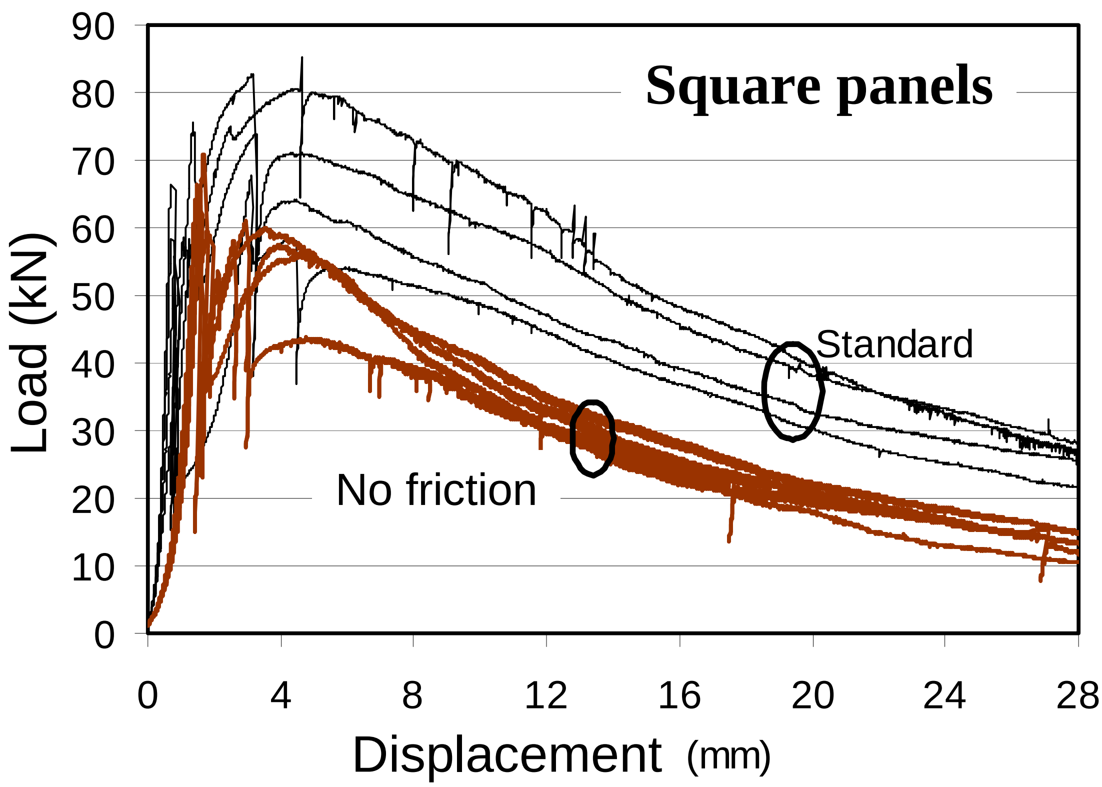

Fig. 6.5 Measured load-deflection curves for all square panels.

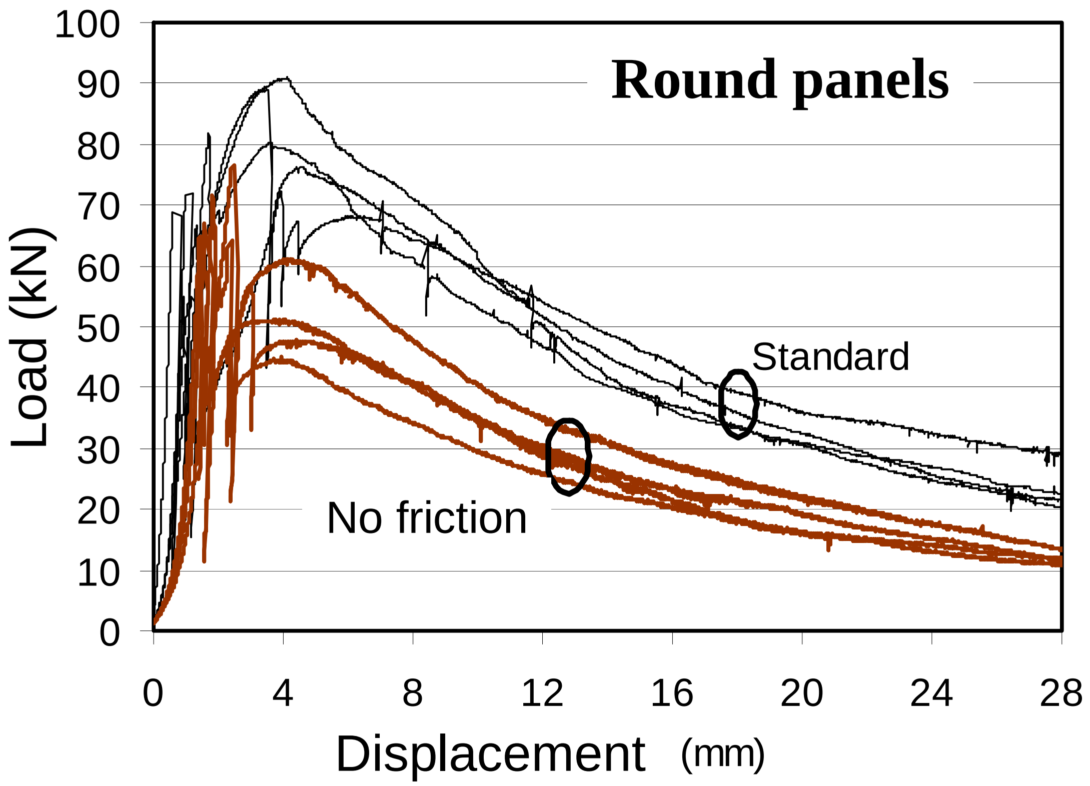

Fig. 6.6 Measured load-deflection curves for all round panels.

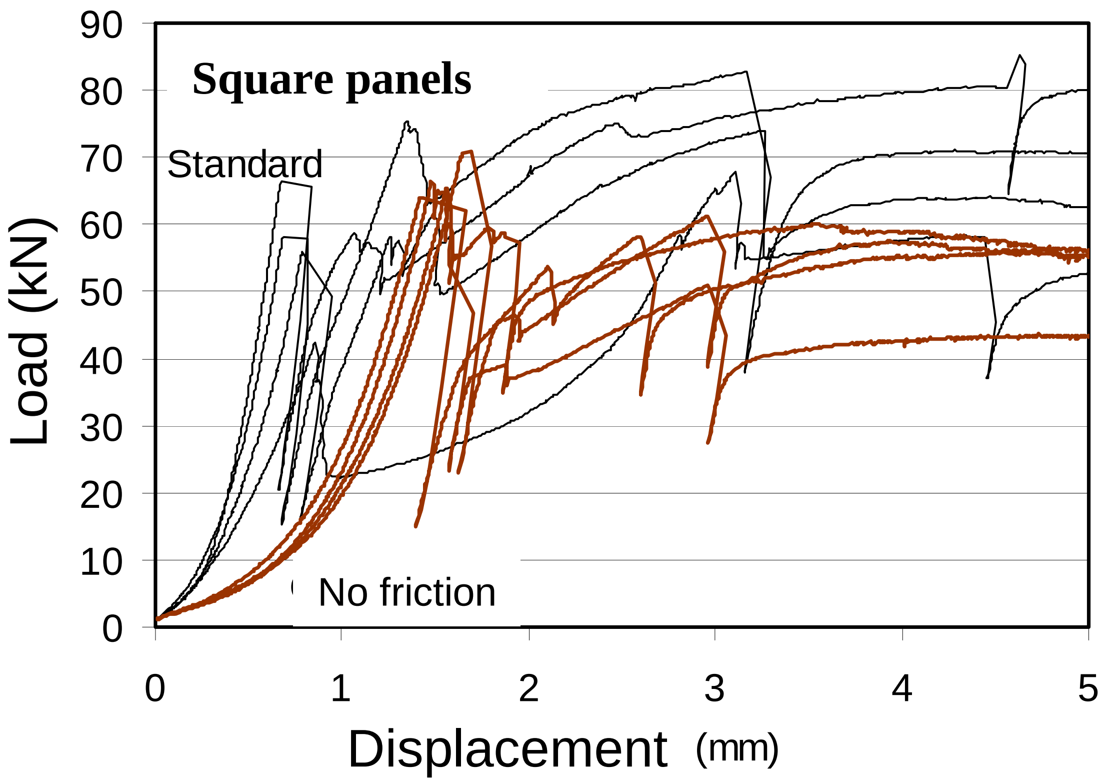

Fig. 6.7 Early load-deflection development for all square panels.

Fig. 6.8 Example, “no friction” conditions: Lifting of panel edge, opening of a crack and sliding (in the grease layer) along the inner edge (not visible) of the support. Sliding takes place between the cut upper plastic sheet layer (blue) and the plastic layer below (grey).

6.6.3 Effect of panel geometry

For similar friction conditions the energy absorption capacity from the square and the round panel tests obtained quite similar average results:

For “standard” conditions the average results became:
Square panels = 1158 J and Round panels = 1153 J
Hence, relation Square/Round panels = 1158/1153 = 1.00

For “no friction” conditions the average results became:
Square panels = 765 J and Round panels = 726 J
Hence, relation Square/Round panels = 765/726 = 1.05

6.7 Effect of friction on maximum load and residual strength

Maximum load during the test and the residual strength (load) at 25 mm (corrected) central deflection versus energy absorption capacity are show in Fig. 6.9 (single results) and Fig. 6.10 (average results). The trend is that higher values for the two parameters means increasing energy absorption capacity, which is not very surprising considering that the energy uptake is calculated as the area below the load-deflection curve, and high loads means more energy.

It is clear that highest maximum loads and residual strengths (open dots in the figures) are associated with “standard” condition tests. This means that the friction not only work to resist the opening of the cracks in the post-cracking phase, but it also appears that the restraining effect by friction to radial sliding at the support increases flexural strength of the concrete panel in the pre-cracking phase. Remember that all tests are on panels that are made with the same concrete mix.

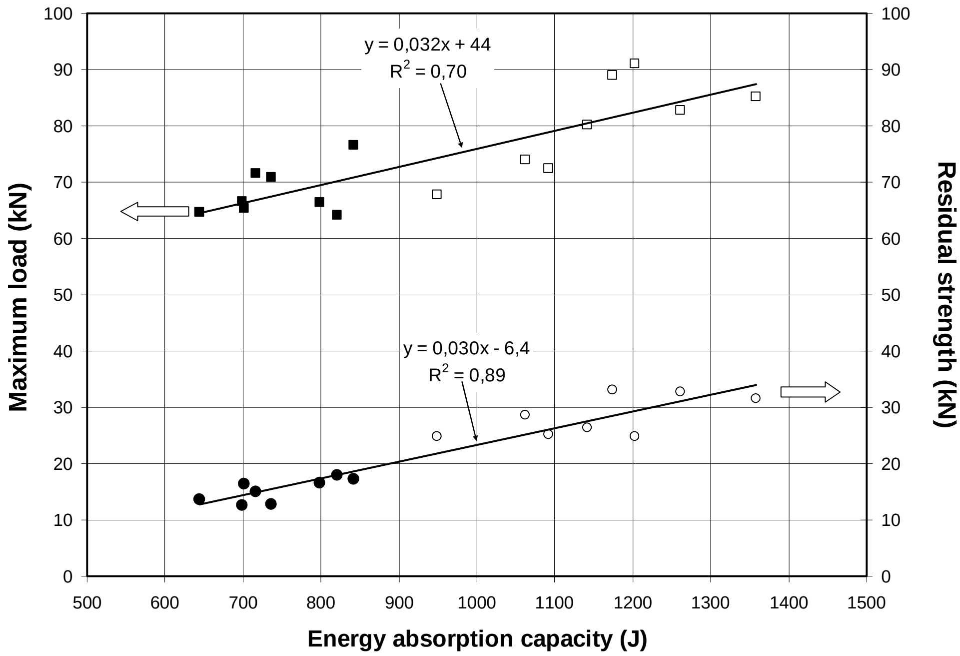

Fig. 6.9 Single results: Maximum load and residual strength (at 25 mm central deflection) versus energy absorption capacity. Filled black dots are for panels with "no friction" conditions, while open dots are for panels with "standard" conditions.

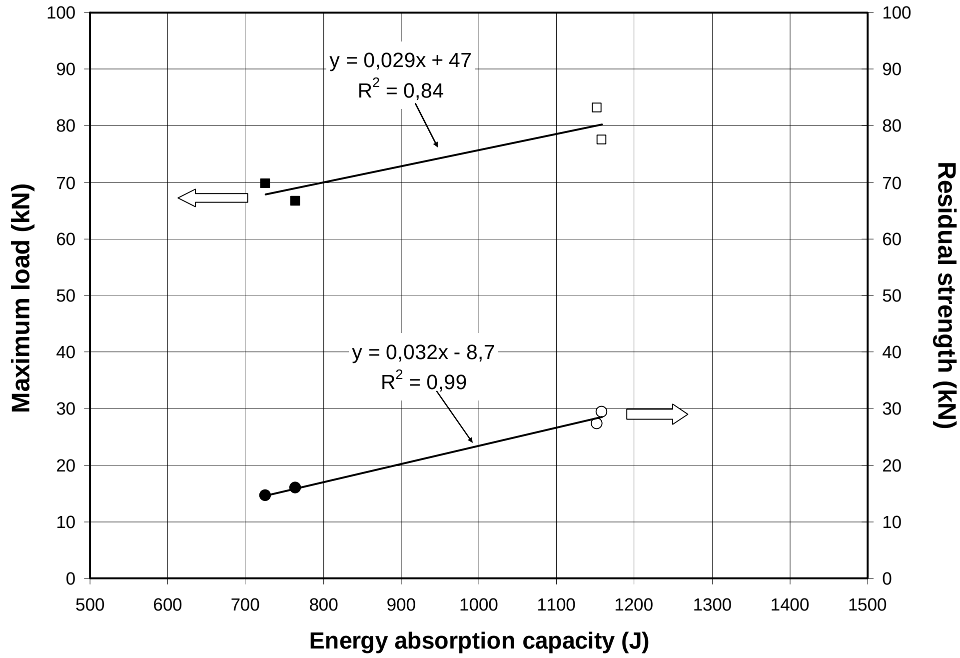

Fig. 6.10 Average results for each set: Maximum load and residual strength (at 25 mm central deflection) versus energy absorption capacity. Filled black dots are for panels with "no friction" conditions, while open dots are for panels with "standard" conditions.

On average the maximum load for the panels with "no friction" conditions is 85 % compared to the panels with "standard" conditions. An interesting feature here is also that the deflection level at the point of maximum load is much lower for the "no friction" conditions. On average the measured deflection at maximum load is 1.7 mm in the "no friction" tests, while it is 3.7 mm in the "standard" tests. The low 1.7 mm deflection for "no friction" conditions occurs despite of the fact that these tests have more pronounced non-linear behaviour in the very early loading branch, probably due to compression of the plastic sheet layers, which in itself contributes to extra (and erroneous) displacement. Note that the early non-linear behaviour does not influence the overall energy absorption capacity from the tests, see Chapter 7.

For the residual strength at 25 mm deflection the effect of friction appears to be substantial. On average, the results show that the residual strength for the "no friction" tests is only 54 % compared to the "standard" tests.

The average between the (100-85=) 15% friction effect on maximum load and the (100-54=) 46% friction effect on residual strength is 31%. This is not far from the overall 35% friction effect that is proven for the normal ("standard") energy absorption capacity tests. This correspondence is not surprising since the load is quite linear between maximum load and the residual load at 25 mm displacement, and the energy is calculated as the area below.

Coefficient of variation (COV) for maximum load is 6.3 % among all the "no friction" tests and 10.3 % among all the "standard" tests. For residual strength the COV is around 13 % for both test conditions.

7 Average results and adjustment for early non-linear behaviour

7.1 General

In this chapter the average results are evaluated in order to study the effect of friction over the whole deflection span between zero and 25 mm, and not only for the overall effect after 25 mm deflection as discussed in the previous chapter. To enable this all load-deflection records are "normalized" with regard to panel thickness. Within each set (four panels) this enables a summarizing and averaging of the results over the deflection span. The normalizing procedure is described in the following Section 7.2 and the average results are presented thereafter (Section 0).

The averaged results are then adjusted for the early non-linear behaviour (Section 7.4). The non-linear behaviour is likely to be attributed to early testing disturbances since it is expected that concrete in the pre-cracking stage should behave elastic (linear). For the "no friction" condition the non-linearity is particularly clear, probably due to squeezing of the plastic sheets during early loading. In the ASTM-panels with 3-points support [13] the early non-linearity can apparently be attributed to some crushing of the concrete by the point-loads at the support, but such crushing was not observed in the present tests. Finally, the effect of the adjustments on calculated energy absorption is discussed, as well as the effect of friction over the whole 0-25 mm deflection span.

7.2 Normalizing the load-deflection record

The following discussion applies the assumptions in Section 5.4.4 for correction of results in terms of panel thickness. Assuming a load-displacement behaviour within the deflection increment Δ_i to Δ_{i+1} for a panel with thickness > 100 mm as shown in Fig. 7.1. The energy (E_i) between Δ_i and Δ_{i+1}) is then defined by the load-displacement curve and the broken lines, hence:

Equation 15

$$E_i = (\Delta_{i+1} - \Delta_i)\frac{P_i + P_{i+1}}{2}$$

The grey trapezium is then a "normalized" area with regard to panel thickness since the panel would have obtained this behaviour theoretically if it had been 100 mm thick. The energy E_{ik} in the grey trapezium is then given as:

Equation 16

$$E_{ik} = \left(\frac{\Delta_{i+1}}{k} - \frac{\Delta_i}{k}\right)\frac{P_i \cdot k + P_{i+1} \cdot k}{2} = \left(\frac{\Delta_{i+1} - \Delta_i}{k}\right)\frac{(P_i + P_{i+1})k}{2}$$

Remember that k=100/h and h is the panel thickness. Hence, E_{ik} according to Equation 16 up to a displacement of Δ_i/k equals to E_i according to Equation 15 up to a displacement Δ_i. Similarly, if this was the last displacement increment during the test for a panel with thickness>100 mm then Δ_i=25mm$\cdot k$, and Δ_i/k=(25mm $\cdot$ k)/k=25mm. Consequently, different load-deflection curves can then be compared at each given (normalized) deflection level. The equations are also valid for panels with thickness<100 mm. The accumulated energy (EAC) from zero deflection and further on up to a given deflection $\Delta\gamma$ then becomes:

Equation 17

$$EAC = k\sum_{i=0}^{i=\Delta\gamma}\left[\frac{\left(\Delta_{i+1}-\Delta_{i}\right)}{k}\frac{\left(P_{i}+P_{i+1}\right)k}{2}\right]$$

Using this equation different EAC-curves, from panels with different thickness, can be summarized and averaged at all deflection levels.

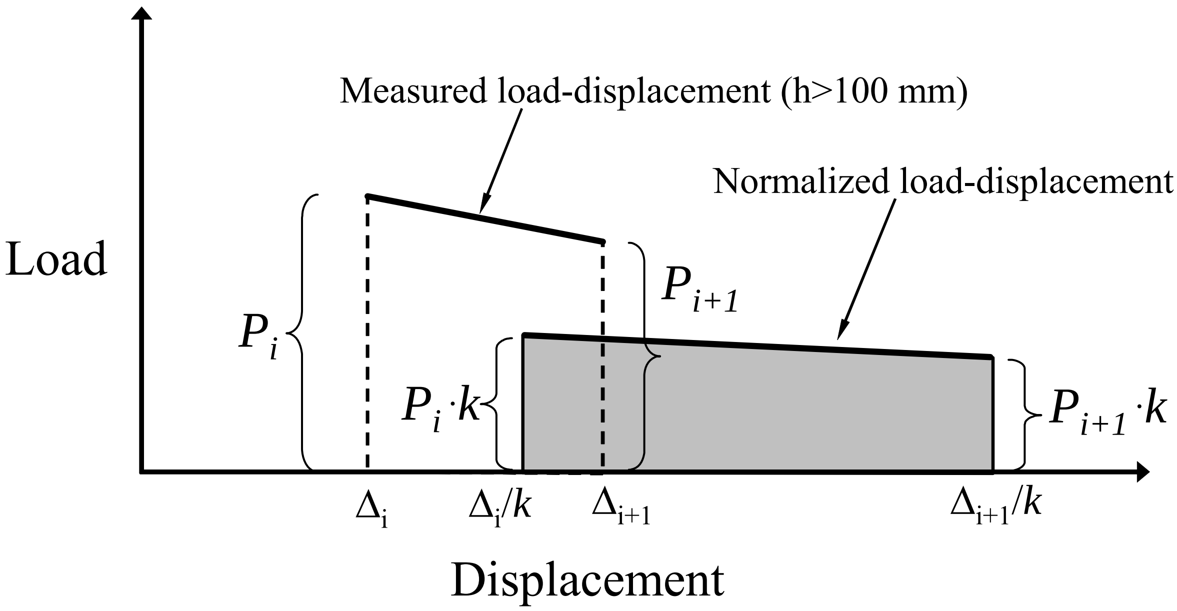

Fig. 7.1 Measured load-displacement in a displacement interval (dotted area) and equivalent/normalized area expressed by the grey trapezium.

7.3 Average results

After normalizing the load-deflection records in terms of panel thickness according to the previous section the results are directly comparable, Fig. 7.2 shows normalized single- and averaged load-deflection curves.

The average results for all four data sets are plotted together in Fig. 7.3, whereas Fig. 7.4 gives the corresponding average accumulated energy (EAC). It can be seen that the very early EAC-development for “no friction” conditions has a slow start which is due to the pronounced early non-linear behaviour in these tests (squeezing of the two layers of plastic sheets). The early difference between “standard” and “no friction” (no fr.) conditions in Fig. 7.4 is eliminated when the curves are adjusted for the non-linearity. This is shown in the following section.

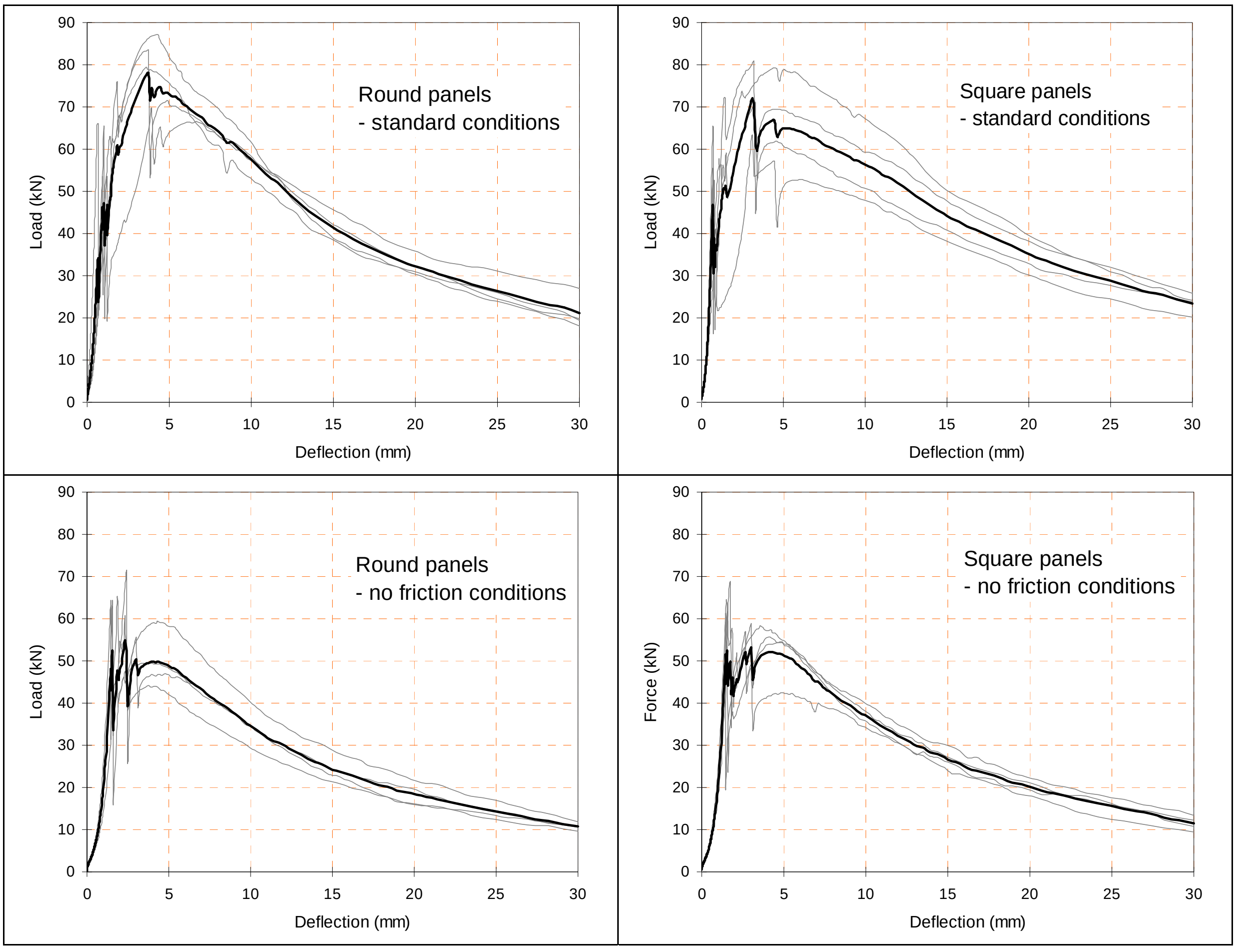

Fig. 7.2 Normalized single load-deflection curves (thin, grey curves) and average curves (thick, black curves) for the four sets. One figure for each test series.

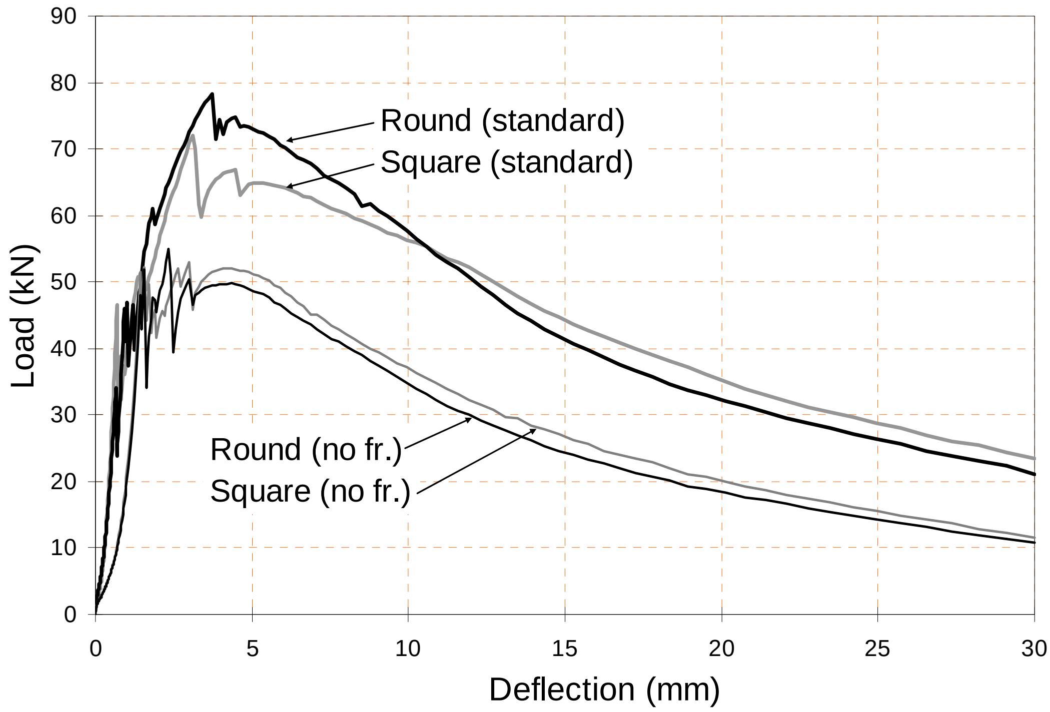

Fig. 7.3 Average load-deflection curves for the four sets.

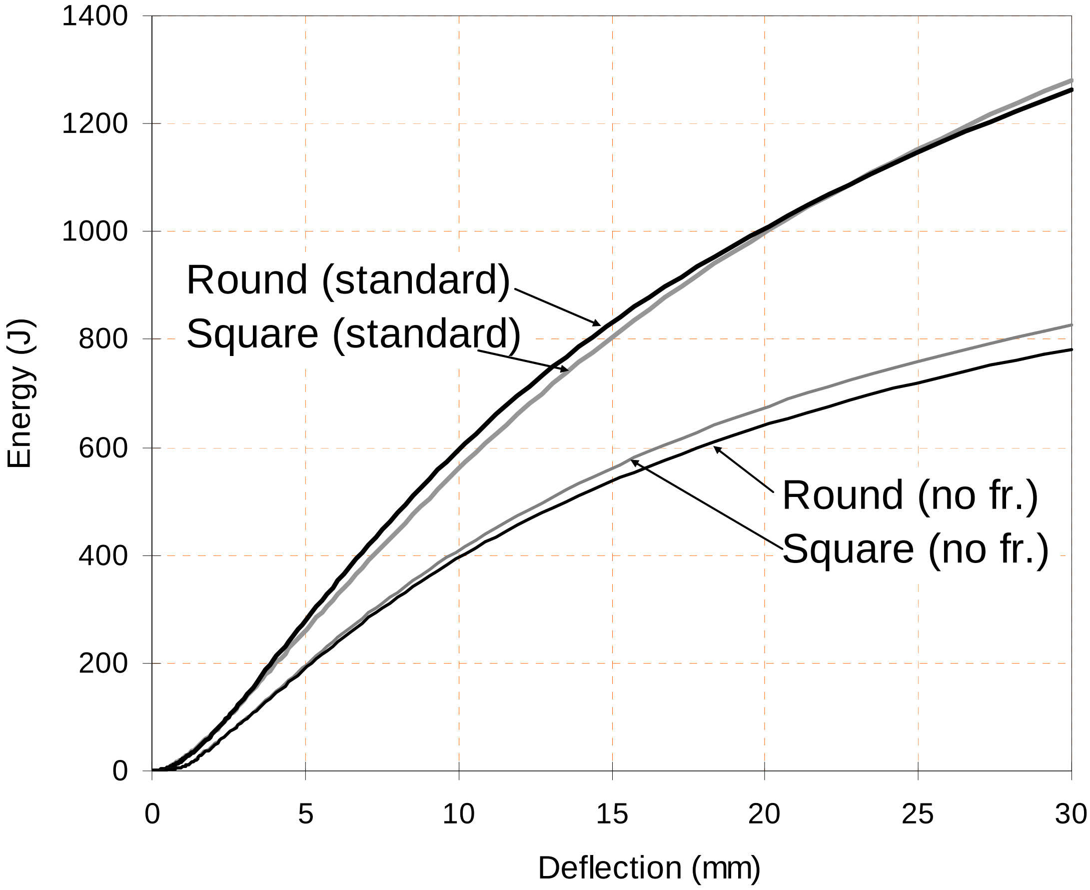

Fig. 7.4 Average energy uptake for the four sets.

7.4 Adjusting the load-deflection curve and effect of friction over time

To adjust for the early non-linear behaviour we need to study this phase closely, see Fig. 7.5. The non-linearity is particularly clear for the “no friction” (no fr.) condition. Pre-cracked concrete is expected to show elastic/linear behaviour; hence from a fundamental standpoint the non-linearity is due to measuring disturbances and should be adjusted for before energy-assessments. A procedure to adjust for this is described in the ASTM-standard for round panels with 3-points support [13].

According to the ASTM-description, the following is done here: The upper linear ascending part of the load-deflection curve is extrapolated back to zero load. The intersection with the deflection-axis gives the offset value. It can be seen from Fig. 7.5 that the offset for “standard” conditions is 0.25 mm and for “no friction” conditions it is 0.8 mm. For simplicity, each couple with similar test conditions is given the same offset. The extrapolation (the broken lines) is then set to be the adjusted result in this early phase. The whole load-deflection curve is then shifted to zero deflection (shifted to the left) according to the offset-value, hence some early energy (area) from the original curves will be eliminated due to the procedure. For the two “no friction”-curves the eliminated early energy is indicated by the dotted lines, which for the given case constitutes 7 Joule.

The final adjusted load-deflection curves are shown in Fig. 7.6 and the corresponding accumulated energy in Fig. 7.8. The latter figure shows that the very early difference in energy for the two test conditions is not there anymore. However, the overall energy uptake (from zero to 25 mm deflection) was only to a minor degree affected by the adjustment procedure (compared to the unadjusted results, Section 6.6). There was actually a small increase of the total energy up to 25 mm deflection when adjusting for the early non-linear behaviour despite the fact that early energy is eliminated by the procedure (7 Joules was eliminated for the “no friction” condition). The reason for this is simply that the energy that is gained beyond 25 mm deflection more than compensates for the early energy elimination. For example, when shifting the “no friction” curves by an offset of 0.8 mm the part of the curve between 25 mm and 25.8 mm in the original data set is then included in the adjusted energy calculation (gives an addition of around 12 Joules). Similarly, for the “standard”-curves the part of the curve from 25 mm to 25.2 mm (offset was 0.2 mm) is included. The net result is that the adjustment procedure generates an increase of 0.6-0.7 % in the total energy for the “no friction” condition and 0.3-0.4 % for the “standard” condition. In other words, among the given results the total energy from zero to 25 mm deflection was by no means significantly affected by compensating for the early non-linear behaviour.

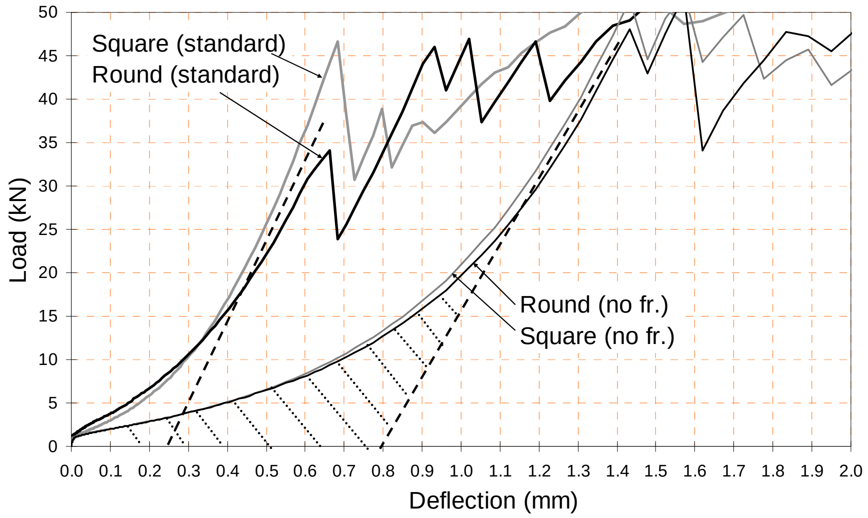

Fig. 7.5 Average curves for the four sets. Extrapolation (see broken line) of the linear part of the pre-cracking branch of the load-deflection curve. Offset for “standard” condition = 0.25mm and for no friction conditions “(no fr.)” = 0.8mm.

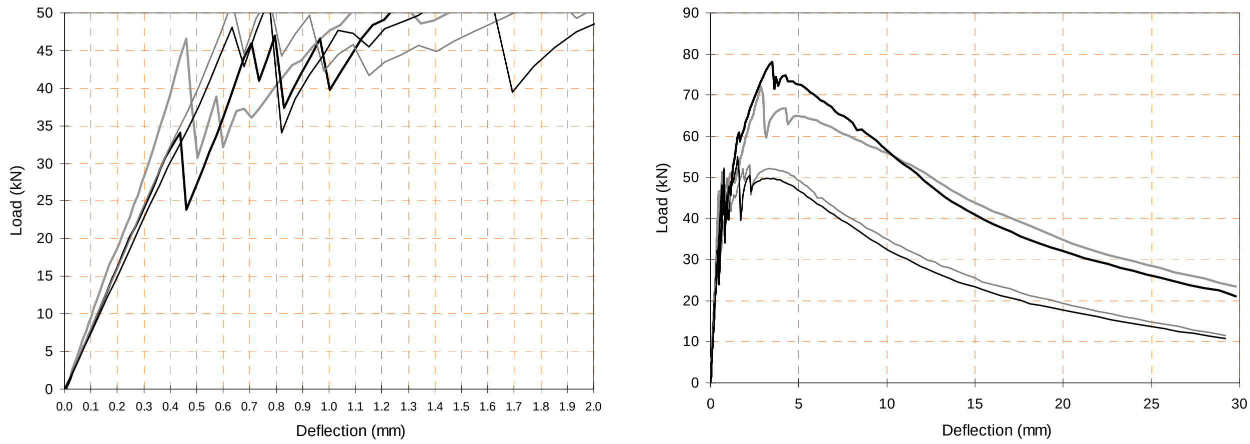

Fig. 7.6 Average load-deflection curves after moving the curves to zero start-point according to the offset values. Early period (left) and the whole period (right).

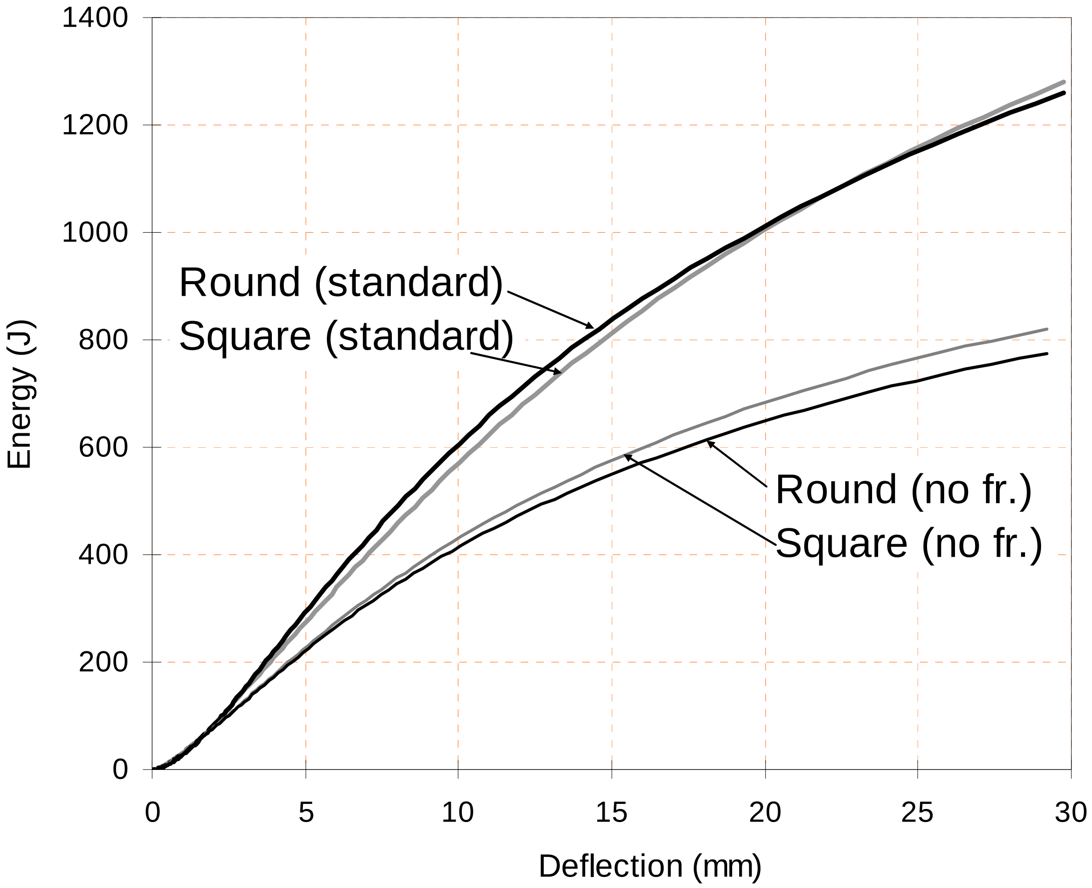

Fig. 7.7 Average energy absorption capacity curves for the four sets after adjusting for the early non-linear behaviour.

Nevertheless, the data sets have now normalized deflection-axes and we assume that the disturbances by the early non-linear feature have been eliminated. The overall friction effect over the whole deflection span can now be evaluated: <u>The ratio</u> between the energy uptake for “no friction”- and “standard” condition versus central deflection (Δ) is shown in Fig. 7.8. The two energy curves from each test condition have been averaged in the calculation. The effect of friction and fibre action is indicated in the figure.

A constant ratio of 1.0 would indicate that there was no friction effect, but this is indeed not the case. It is clear that the effect of friction increases with increasing deflection and that the overall friction effect at 25 mm deflection is 35 %, which is the same as discussed earlier in Section 6.6.2. The implication is that the coefficient of friction increases during the test.

Increased deflection means larger and more rotated crack openings which maybe gradually lead to more distinct point-contact between the panel and the support. The result might be that the crack edges gradually penetrate the wooden support ring in the “standard” set-up. If this is the case it is likely that the coefficient of friction increases.

At low deflection levels (in the pre-cracking phase) the ratio shows an irregular behaviour. This is partly due to the sensitivity of dividing small numbers by each other and probably also due to the early (manual) adjustments of the load-deflection curves. The different crack propagation behaviour for the two support conditions will also contribute. As more energy is accumulated the curve in Fig. 7.8. becomes more “robust”.

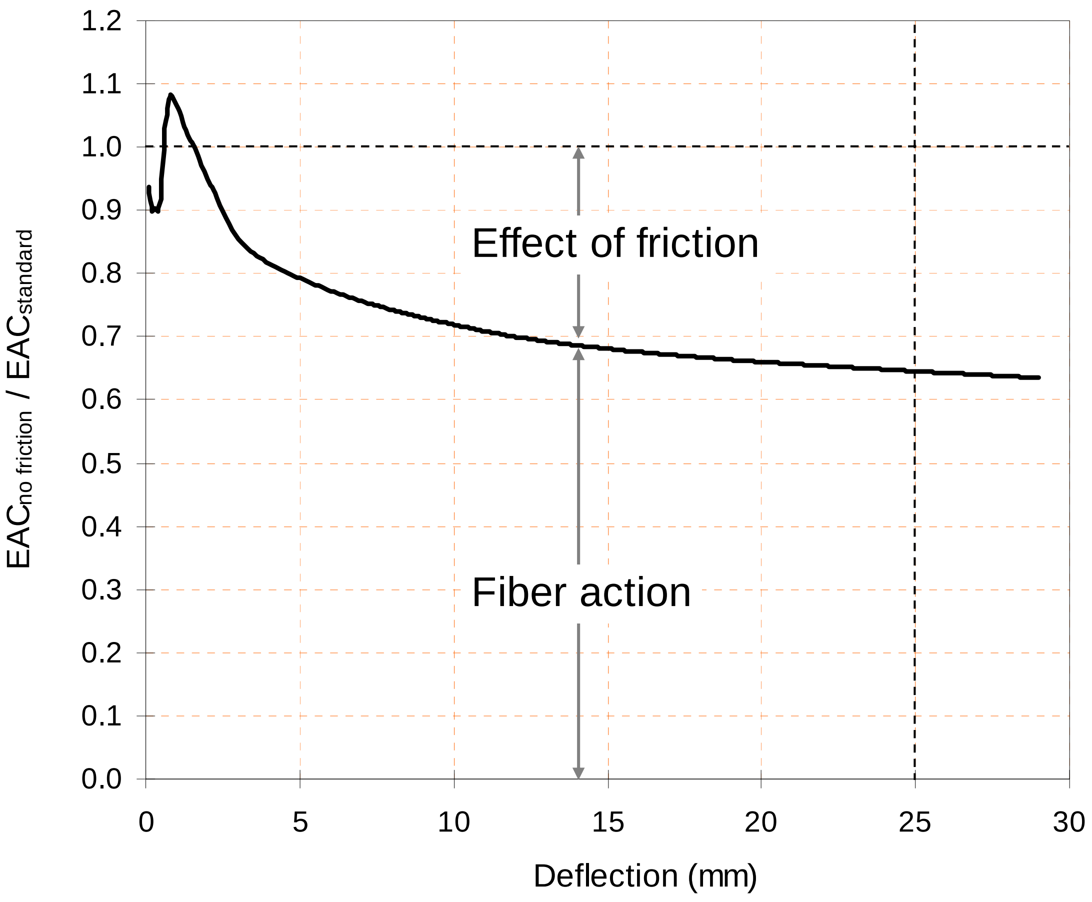

Fig. 7.8 Relation between the average energy absorption capacity (EAC) for the two sets of "no friction" conditions and the two sets of "standard" conditions.

8 Calculation of friction energy and coefficient of friction

Based on the average results from the previous chapter the coefficient of friction (μ) is calculated here. The calculation assumes that there was no friction in the tests denoted “no friction” test, and that the results then represent the inner work (W_i) of the panels. The energy from the “standard” condition tests ($EAC_{standard}$) is calculated as the work from the external load P (i.e. W_P).

When using Equation 2 and Equation 12 from Chapter 2 the friction work (W_F) and can be calculated as:

Equation 18
$$W_F = \sum_{\Delta=0}^{25mm} \mu_\Delta P_\Delta dw_F = \sum_{\Delta=0}^{25mm} \mu_\Delta \frac{(P_i + P_{i+1})}{2} \sqrt{\left(\frac{\Delta \cdot h}{L'}\right)^2 + \left(\frac{h}{L'}\left[\Delta - \frac{\Delta^2}{2h}\right]\right)^2}$$

and

Equation 19
$$EAC_{no\_friction} = EAC_{standard} - W_F$$

The only unknown in Equation 19 is μ, hence μ can be deduced from the test results by using the iteration and the least square root principle. In the first iteration the coefficient of friction (μ) was set to be a constant value. Best fit between measured- ($EAC_{no\_friction}$) and calculated inner work ($EAC_{standard}$ - W_F) was obtained for $\mu = 0.58$, see Fig.8.1. It can be seen that the correspondence with the measurement is quite good with this constant μ. For friction between wood and steel (clean and dry surfaces) the value $\mu = 0.62$ for static friction is given in [15] (no kinetic coefficient is given); this is very close to the constant value found here. The interaction between static and kinetic friction during the panel tests is unclear, but the drops in load at rather high deflection levels may indicate that the friction alternate between the two types of friction.

As already discussed the results indicate directly that the friction effect increase with the deflection level. In the second iteration μ was therefore expressed by the following linear model:

Equation 20
$$\mu(\Delta) = a \cdot \Delta + b$$

where a and b are fitting parameters and Δ is the central deflection.

Best fit was obtained for a=0.031 and b=0.33. It can be seen, see Fig. 8.2, that the correspondence improved in terms of agreement to the measured curve, confirming that μ increase with the deflection – and it appears to be very high towards the end of the test! The accuracy of the test method (COV≈10%) and the limited amount of tests, however, demands for caution with regard to drawing to distinct conclusions on the absolute level(s) of μ.

The friction condition in the pre-cracking period at low displacement is somewhat uncertain, as discussed in the previous section, and it differs from that of the post-cracking period for which the calculations are most relevant. Thus, the calculation of μ from zero up to some mm deflection is uncertain; this period is indicated with grey area in the figure.

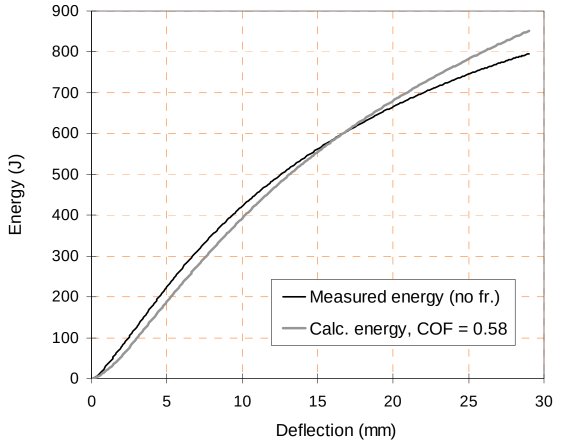

Fig. 8.1 Best fit between calculated- and measured inner energy from the "no friction" tests. The calculation is based on a constant coefficient of friction (COF).

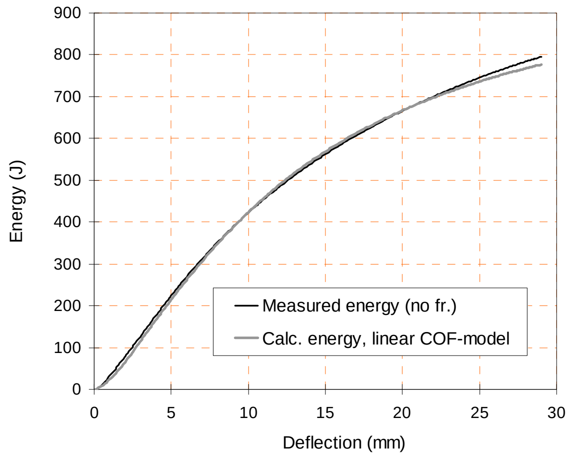

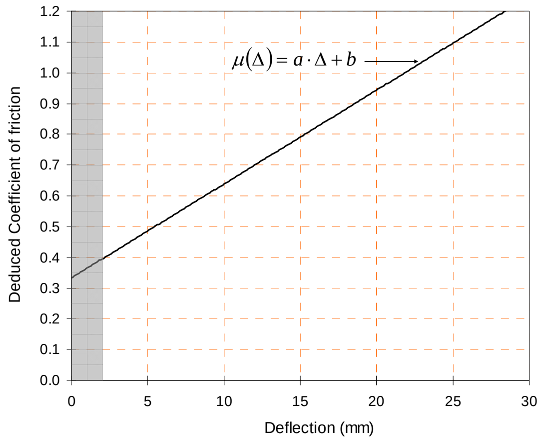

Fig. 8.2 Left: Best fit between calculated- and measured inner energy from the "no friction" tests. The calculation is based on a linear model for the coefficient of friction (COF). Right: The development of COF that gave the best fit (*a*=0.031 and *b*=0.33). Grey area indicates the pre-cracking period.

9 Conclusions and final remarks

The potential effect of friction is the same for round and square panels, presuming that the support material is the same. It is assumed that four perpendicular cracks form and that the cracks are oriented normal to the support. The theoretical evaluation shows that the effect of friction will be somewhat less for square panels if the cracks are oriented closer to the corners.

The energy absorption capacity (EAC) test results show that the average coefficient of variation (COV) was 7.8 % for the two individual sets of round panels and, similarly, 11.7 % for the square panels. The average COV for EAC for the two different friction conditions were quite similar.

The EAC from square and round panels with similar support (friction) conditions corresponded well.

In panel tests with continuous support the friction occurs in two directions; tangential and radial. The tangential- and radial movements of the panel relative to the support have been quantified.

The results show that the friction conditions between the concrete panel and the support fixture has a great impact on the measured energy uptake. For the case denoted “standard” conditions, which is the normal set-up for panel tests, the results show that 35% of the overall energy uptake between zero and 25 mm deflection is due to friction, and the remaining 65% is due to fibre action in the concrete panel.

When friction is eliminated in the test, the results show, on average, that the maximum load during the test is reduced by 15 % and the residual load at 25 mm deflection is reduced by 46 %.

By using the energy balance equations the coefficient of friction was deduced from the test results. It is found that the coefficient of friction is substantial and that it increases as the test proceeds. This may be associated with a gradual penetration of the sharp concrete crack edges into the wooden support.

Adjustments of the early non-linear behaviour of the load deflection curves have been made in accordance to the procedure in ASTM 1550-05. The adjustments had no significant effect on the calculated energy absorption capacity.

The effect of friction in panel tests with steel support is not investigated here, and, to our knowledge, not investigated elsewhere either. Coefficient of friction values in the literature ([10], [15]-[17]) indicate that there is no reason to believe that the effect of friction with steel support should be any less than shown in this report for wooden support. Using a bedding material on top of the support fixture (as described in EN 14488-5 for steel support) probably also has an effect, but to which extent is uncertain.

10 References

[1] Norwegian Concrete Association's publication no. 7: "Sprayed concrete for rock support". 2003 (in Norwegian, title: Norsk Betongforenings publikasjon nr. 7: "Sprøytebetong til bergsikring")

[2] NS-EN 14488-1 Testing sprayed concrete, Part 1. Sampling fresh and hardened concrete. 2005

[3] NS-EN 14488-5 Testing sprayed concrete, Part 5. Determination of energy absorption capacity of fibre reinforced slab specimens. 2006

[4] Handbook 014 Laboratory investigations. Guidelines. The Norwegian Public Roads Administration, Des. 1997 (in Norwegian: Håndbok 014 Laboratorieundersøkelser. Rettningslinjer, Statens vegvesen, des. 1997)

[5] NS-EN 14488-7 Testing sprayed concrete. Part 7: Fibre content of fibre reinforced concrete. 2006

[6] Bernard E.S. (2001) The influence of strain rate on performance of fiber-reinforced concrete loaded in flexure. Cement, concrete and aggregates, CCAGDP, Vol.23, No.1, June 2001, pp. 11-18

[7] Myren S.A. and Bjøntegaard Ø. (2008) Energy absorption capacity for fibre reinforced sprayed concrete. New test rig, effect of panel geometry and testing laboratory (Series 1). Technology report no. 2531, Norwegian Public Roads Administration, Road Directorate. 2008-10-16 (in Norwegian, title: Energiabsorpsjonskapasitet for fibrearmert sprøytebetong. Ny forsøksrigg, effekt av plategeometri og testlaboratorium (Runde 1))

[8] Bjøntegaard Ø. and Myren S.A. (2008) Energy absorption capacity for fibre reinforced sprayed concrete. Effect of panel geometry and fibre content (Series 2). Technology report no. 2532, Norwegian Public Roads Administration, Road Directorate. 2008-10-24 (in Norwegian, title: Energiabsorpsjonskapasitet for fiberarmert sprøytebetong. Effekt av plategeometri og fiberinnhold (Runde 2)).

[9] Myren S.A. and Bjøntegaard Ø. (2009) Energy absorption capacity for fibre reinforced sprayed concrete. Effect of panel geometry, fibre content and fibre type (Series 3). To be published in 2009

[10] Bernard E.S. (2005) The Role of Friction in Post-Crack Energy Absorption of Fibre Reinforced Concrete in the Round Panel Test. Journal of ASTM International, January 2005, Vol. 2, No. 1

[11] Thorenfeldt E. (2006) Fibre reinforced concrete panels. Energy absorption capacity for standard samples. SINTEF memo (in Norwegian, title: Fibrearmerte betongplater. Energiabsorpsjon for standard prøver).

[12] Bjøntegaard Ø. (2008) Testing of energy absorption for fibre reinforced sprayed concrete. Proc. of the 5th Int. Symp. on Sprayed Concrete – Modern use of wet sprayed concrete for underground support. Lillehammer, Norway, 21-24 April 2008, pp. 60-71, ISBN 978-82-8208-005-7. Tekna, Norwegian Concrete Association.

[13] ASTM C1550-05 Standard Test Method for Flexural Toughness of Fibre Reinforced Concrete (Using Centrally Loaded Round Panel)

[14] DiNoia T.P. and K.-A. Rieder (2004) Toughness of reinforced shotcrete as a function of time, strength development and fibre type according to ASTM C1550-02. Shotcrete: More Engineering Developments – Bernard (ed.), 2004 Taylor & Francis Group London, ISBN 04-1535-898-1, pp. 127-135

[15] Cook R.A. (1989) Behavior and design of ductile multiple-anchor steel-to-concrete connections. Ph.D thesis, Univ. of Texas at Austin, May 1989.

[16] Funk R.R. (1989) Shear friction mechanisms for support attached to concrete. Concrete International, July 1989, pp. 53-58

[17] Kurtus R. (2005) Coefficient of Friction Values for Clean Surfaces, www.school-for-champions.com/science/friction_coefficient.htm

APPENDIX 1 Mixing log from the plant

Unicon AS

Blanderapport

v. 1.13
Side 1 d. 21-05-2008 kl. 14:26:03

Nummer..: 2008040420071 Sjursøya2

Bestillingsnr. ......: 408728 Recept ....: 55830A
Kundenummer ...: 100015
Kunde ....: Entreprenørservice As, Rud
Rudsletta 24
1351 RUD

Ønsket konsistens ...: 200
Blandemester ....: guda
Blander ....: Fabrikk2
Bilnr. ....: 612

Adresse ....: E-6 Ved Ringnes Tunellen
1415 OPPEGÅRD

Fabrikk ....: Sjursøya2 Produceret (m3) .: 6,02
Følgebrev ....: 363865 Blandedato ....: 04-04-2008
Blandetidspunkt .: 09:40:37

Sammensætning	Materialenavn	Fugt %	Densitet kg/m3	Tilsat (bør)	Blandet kg	1 m3 (bør)	V.O.T. er
Pumpeforbedrer	tcc 735 n	75,0	900	27	27	4,5	4,5
Kort stålfiber	Dramix 65/35		7.850	120	120	20	20
Sement	Norcem Anlegg		3.120	1.348	1.347	225	224
Sement	Norcem Std FA CEM II/A-V 42,5R		2.950	1.354	1.359	226	226
Silika	Silikastøv k=2		2.200	134	135	22	22
Sand	0-8 mm Svelviksand	2,0	2.672	9.622	9.638	1.572	1.571
SP-stoff	Glenium SKY 552	81,0	1.050	25	25	4,1	4,2
Retarder	Delvocrete Stab	81,5	1.100	8,9	8,9	1,49	1,48
Luftinnførende stoff	MICRO AIR 100 (1:19) BASF	99,4	1.000	5,6	5,6	0,94	0,93
Vand	Kaldt vann		1.000	886	884	148	147
Vand	Varmt vann		1.000	118	118	20	20
Vand	Vand		1.000	2,0	11	0,33	1,83
	Total: Fugt i materiale		1.000	0,00	0,00	31	31
		Total kg		13.650	13.679	2.275	2.274
		Volumen (liter)		6.000	6.016	1.000	1.000

	Bør-verdi	Målt / bereg.	
Total vand ....:	208,0	208,7	l/m3
Ækvivalent cement ....:	495,0	494,7	kg/m3
Ækv. V/C-forhold ....:	0,42	0,42	
Konsistens ....:	200		mm
Blandetid ....:	60,00	54,50	s
Rumvægt ....:	2.275	2.274	kg/m3
Luftindhold i % af beton ....:	4,0		%
Luftindhold i % af kitmasse ....:	9,7	9,7	%

Kornkurve, gennemfald i %

Sigte, mm	0,063	0,125	0,25	0,5	1	2	4	8	11	16	22	32
Vægt % (Bør)	0	3	9	28	52	72	88	100	100	100	100	100
Vægt % (Er)	0	3	9	28	52	72	88	100	100	100	100	100

APPENDIX 2 Fibre, product data sheet

PRODUCT DATA SHEET BEKAERT

Dramix®

R | C | -65/35- | B | N
Low Carbon

• Description:

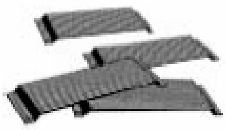

Dramix® fibres are filaments of wire, deformed and cut to lengths, for reinforcement of concrete, mortar and other composite materials. Dramix® RC-65/35-BN is a cold drawn wire fibre, with hooked ends, and glued in bundles.

• Applications:
- shotcrete
- screeds
- precast
- overlays
- compression layers

• Geometry:

Length (l) 35 mm

Diameter (d) 0,55 mm

65 — Performance class: 65

Aspect ratio (= l/d): 64

14 500 fibres/kg

• Tensile strength:
- on the wire: minimum 1100 N/mm²
- low carbon conforms to EN 10016-2 - C9D

• Coating: None

• Approvals:

Conforms to ASTM A820

Quality System in Belgian, Brasilian, Czech, Turkish and Chinese plants — ISO 9001

Product		Product	
Belgium	ATG 04/1857	Poland	AT-15-2117/2001
Turkey	TS 10513	Romania	007-01/068-2003
Germany	Z-3.71-1745	Slovak Republic	1402A/02/0771/1/C/C04
Czech Republic	C.070-021415		

• Technical data:
For shotcrete, ... ask for specialized documentation

Recommendations - mixing

1. General
✓ preferably use a central batching plant mixer
✓ recommended maximum dosage:

Max. aggregate size (mm)	Dosage (kg/m³) pour	Dosage (kg/m³) pump
8	110	80
16	70	55
32	60	45

✓ a continuous grading is preferred
✓ mix until all glued fibres are separated into individual fibres. Fibres don't increase mixing time significantly.
✓ if special cements or admixtures are used, a preliminary test is recommended

2. Fibre addition
Bags are non-degradable and may not be thrown into the concrete.

2.1. In batching plant mixer
✓ never add fibres as first component in the mixer
✓ fibres can be introduced together with sand and aggregates, or can be added in freshly mixed concrete

2.2. Truckmixer
✓ run mixer at drum speed: 12-18 rpm
✓ adjust slump to a min. of 12 cm (preferably with water reducing agents or high water reducing agents)
✓ add fibres with maximum speed of 60 kg/min
✓ optional equipment: belt-hoist elevator
✓ after adding the fibres, continue mixing at highest speed for 4-5 min. (± 70 rotations)

2.3. Automatic dosing
✓ Fibres can be dosed from bulk at rates from 0 up to 3,5 kg/sec with a specially developed dosing equipment

Recommendations - storage

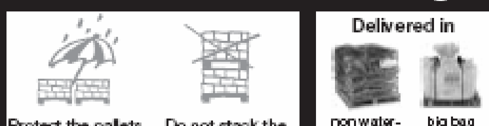

Protect the pallets against rain

Do not stack the pallets on top of each other

Delivered in: non water-soluble bags of 20 kg on pallet 1 200 kg; big bag 1100 kg

N.V. Bekaert S.A. - Bekaertstraat 2 - 8550 Zwevegem - Belgium
Tel. +32 (0) 56 / 76 69 86 - Fax +32 (0) 56 / 76 79 47
Internet: http://www.bekaert.com/building

APPENDIX 3 Plastic layers, product data sheets,

Product Data Sheet
Edition 18/07/2007
Identification no:
02 07 04 02 002 0 000011 / 15
Mipoplast®-0815/5, 1.50 mm

(Template for local translation, only for internal use)

Construction

Mipoplast®-0815/5, 1.50 mm

Sheet waterproofing membrane

Product Description	Mipoplast®-0815/5 is a homogenous sheet waterproofing membrane, based on polyvinylchloride (PVC-P)
Uses	■ Waterproofing of prefabricated components for small and medium sized swimming pools ■ Pre-formed and transportable pools (i.e. children's paddling pools)
Characteristics / Advantages	■ High resistance to ageing ■ High tensile strength and elongation ■ UV-stabilised ■ Hyginic and resistant to algal growth ■ Resistant to chlorinated water and common swimming pool cleaning chemicals ■ High water vapour transmission ability ■ Resistant to permanent water temperatures of +30°C ■ High dimensional stability ■ High flexibility in cold temperatures ■ Hot air and solvent weldable
Tests	
Approval / Standards	Complies with DIN 16 938.
Product Data	
Form	
Appearance / Colours	Rolled sheet membrane, unreinforced. Surface: smooth Membrane thickness: 1.50 mm Colour (standard): blue (2553), other colours available on request.
Packaging	Roll size: 1.80 m (roll width) x 25.00 m (roll length). Unit weight: 1.84 kg/m²
Storage	
Storage Conditions / Shelf-Life	Rolls must be storaged in their original package, in horizontal position and under cool and dry conditions. They must be protected from direct sunlight, rain, snow and ice, etc.

1 Mipoplast®-0815/5, 1.50 mm 1/3

Technical Data

Chemical Base	Plasticized polyvinylchloride (PVC-P)	
Thickness	0.80 mm	(DIN 53353)
Water Vapour Diffusion Resistance	< 20'000 µ	(DIN 53122)

Mechanical / Physical Properties

Tensile Strength	Longitudinal and transversal: > 17.00 N/mm²	(DIN 53 455)
Elongation	Longitudinal and transversal: > 300%	(DIN 53 455)
Seam Strength	Cracks occur next to the seam.	(DIN 16726)
Behaviour under Hydrostatic Pressure	Watertight at 4 bar over 72 hours.	(DIN 16726)
Puncture Resistance	Watertight at a drop height of 300 mm.	(DIN 16726) (drop-weight of 500 gms)
Dimensional Change after Storage at +80°C	< 1.50%	(DIN 53377)
Behaviour when Folding in Cold	No cracks at -35°C.	(DIN 53361)

Resistance

Appearance after Storage in Heat	No blistering, cracks or capillaries.	(DIN 53377)

System Information

System Structure

Ancillary Products:

- Sika®-Trocal® PVC - laminated metal sheets Type WB for fixing pieces.
- Sika®-Trocal® PVC - solvent for cold welding.
- Sika®-Trocal® PVC - solution (Type WB), for seam sealing.

Application Details

Substrate Quality	Clean and dry, homogeneous, free from oils and grease, dust and loose or friable particles.

Application Conditions / Limitations

Substrate Temperature	0°C min. / +35°C max.
Ambient Temperature	+5°C min. / +35°C max.
Compatibility	Suitable Substrates Concrete, mortar, galvanised steel, aluminium. Non-Suitable Substrates Impregnated wood, high density Polyethylene and rigid PVC, requires a separation layer of geotextile.

Construction

Application Instructions	
Application Method / Tools	This product is suitable for factory welded waterproofing of prefabricated swimming pool components. Membrane installation and welding procedures are developed according to the individual production specifications of pool components.
Notes on Application / Limitations	This product is not suitable for normal membrane installation works on site.
Value Base	All technical data stated in this Product Data Sheet are based on laboratory tests. Actual measured data may vary due to circumstances beyond our control.
Local Restrictions	Please note that as a result of specific local regulations the performance of this product may vary from country to country. Please consult the local Product Data Sheet for the exact description of the application fields.
Health and Safety Information	For information and advice on the safe handling, storage and disposal of chemical products, users shall refer to the most recent Material Safety Data Sheet containing physical, ecological, toxicological and other safety-related data.
Legal Notes	The information, and, in particular, the recommendations relating to the application and end-use of Sika products, are given in good faith based on Sika's current knowledge and experience of the products when properly stored, handled and applied under normal conditions in accordance with Sika's recommendations. In practice, the differences in materials, substrates and actual site conditions are such that no warranty in respect of merchantability or of fitness for a particular purpose, nor any liability arising out of any legal relationship whatsoever, can be inferred either from this information, or from any written recommendations, or from any other advice offered. The user of the product must test the product's suitability for the intended application and purpose. Sika reserves the right to change the properties of its products. The proprietary rights of third parties must be observed. All orders are accepted subject to our current terms of sale and delivery. Users must always refer to the most recent issue of the local Product Data Sheet for the product concerned, copies of which will be supplied on request.
	It may be necessary to adapt the above disclaimer to specific local laws and regulations. Any changes to this disclaimer may only be implemented with permission of Sika® Corporate Legal in Baar.

Sika Services AG
Tüffenwies 16
CH-8048 Zurich
Switzerland
Phone +41 44 436 40 40
Telefax +41 44 436 46 86
www.sika.com

Roofing

Product Data Sheet
Edition 10-2007
Identification no. 020901011230150000
Version no. 001
Sikaplan®-SGK 1.5 (Trocal® SGK, 1.5 mm)

(Template for local translation, only for internal use)

Sikaplan®-SGK 1.5 (Trocal® SGK, 1.5 mm)

Polymeric sheet for roof waterproofing

Product Description	Sikaplan®-SGK 1.5 (Trocal® SGK, 1.5 mm) is a multi-layer, synthetic roof waterproofing sheet based on premium-quality polyvinyl chloride (PVC) with inlay of glass non-woven and polyester fleece backing.
Uses	Roof waterproofing membrane for exposed flat roofs: ■ Partially adhered by Sika-Trocal C 300 adhesive. ■ Loose laid and mechanically fastened.
Characteristics / Advantages	■ Outstanding resistance to weathering, including permanent UV irradiation ■ High resistance to ageing ■ High resistance to hailstones ■ Resistant to all common environmental influences ■ High resistance to mechanical influences ■ High tensile strength ■ High dimensional stability ■ Excellent flexibility in cold temperatures ■ High water vapour permeability ■ Outstanding weldability ■ Optimized adhesion to substrate by polyester fleece backing ■ Polyester backing provides separation to bitumen surfaces ■ Recyclable
Approval / Standards	■ Polymeric sheets for roof waterproofing according to EN 13956, certified by notified body 1213-CPD-4125/4127 and provided with the CE-mark. ■ Reaction to fire according to EN 13501-1, class E. ■ External fire performance tested according to ENV 1187 and classified according to EN 13501-5: BROOF(t3). ■ Official Quality Approvals and Agrement Certificates and approvals. ■ Monitoring and assessment by approved laboratories. ■ Quality Management system in accordance with EN ISO 9001/14001. ■ Production according to Responsible Care policy of Chemical Industry.

Appearance / Colours	Surface:	slightly structured
	Colours:	
	Top surface:	light grey (nearest RAL 7047) slate grey (nearest RAL 7015)
	Bottom surface:	dark grey
	Top surface of sheet in other colours available on request, subject to minimum order quantities.	
Packaging	Packing unit:	12 rolls per pallet
	Roll length:	15.00 m
	Roll width:	2.00 m
	Roll weight:	63.00 kg
Storage Conditions / Shelf-Life	Rolls must be stored in a horizontal position on pallet and protected from direct sunlight, rain and snow. Product does not expire during correct storage.	

Technical Data

Product Declaration	EN 13956	
Visible defects	Pass	EN 1850-2
Length	15.00 (- 0 % / + 5 %) m	EN 1848-2
Width	2.00 (- 0.5 % / + 1 %) m	EN 1848-2
Straightness	≤ 30 mm	EN 1848-2
Flatness	≤ 10 mm	EN 1848-2
Effective thickness	1.5 (- 5 % / + 10 %) mm	EN 1849-2
Mass per unit area	2.1 (- 5 % / + 10 %) kg/m²	EN 1849-2
Water tightness	Pass	EN 1928
Effects of liquid chemicals, including water	On request	EN 1847
External fire performance Part 1-4	BROOF(t3) <10°/<70°	EN 13501-5
Reaction to fire	E	EN ISO 11925-2 , classification after EN 13501-1
Hail resistance rigid substrate flexible substrate	 ≥ 22 m/s ≥ 30 m/s	EN 13583
Joint peel resistance	≥ 300 N/50 mm	EN 12316-2
Joint shear resistance	≥ 500 N/50 mm	EN 12317-2
Water vapour transmission properties	μ = 20'000	EN 1931
Tensile strength longitudinal (md) * transversal (cmd) *	 ≥ 600 N/50 mm ≥ 600 N/50 mm	EN 12311-2
Elongation longitudinal (md) * transversal (cmd) *	 ≥ 50 % ≥ 50 %	EN 12311-2
Resistance to impact hard substrate soft substrate	 ≥ 700 mm ≥ 1500 mm	EN 12691
Tear strength longitudinal (md) * transversal (cmd) *	 ≥ 150 N ≥ 150 N	EN 12310-2
Dimension stability longitudinal (md) * transversal (cmd) *	 ≤ |0.3| % ≤ |0.3| %	EN 1107-2
Foldability at low temperature	≤ -25 °C	EN 495-5
UV exposure	Pass (> 5'000 h)	EN 1297

*md = machine direction
*cmd = cross machine direction

APPENDIX 4 Measurements of panel thickness

All values in mm.

Standard procedure

	Square				Round			
Panel no.	15	9	7	11	6	8	12	10
Measured over the yield lines	101.8	100.7	104.8	102.1	101.6	100.3	103.1	105.9
	101.5	101.8	105.5	104.1	103.4	102.1	105.5	102.3
	101.9	101.0	102.0	104.0	101.0	104.9	105.9	101.8
	100.8	102.8	103.4	103.0	99.9	109.0	109.0	101.4
	101.1	99.2	102.9	102.3	97.9	101.1	104.2	102.8
	100.8	102.0	104.3	101.7	100.9	103.3	106.6	105.9
	101.4	102.9	105.1	102.7	101.9	104.1	107.5	102.1
	101.2	102.6	103.8	102.9	102.0	102.8	106.5	102.4
	101.9	102.2	103.6	103.7	101.7	110.0	107.7	101.7
	101.2	102.1	104.0	102.6	102.2	104.8	107.9	101.1
	101.9	102.4	103.9	102.1	101.9	102.5	108.1	102.7
	101.9	103.5	103.6	103.2	102.7	104.9	110.7	101.5
		103.2	102.9	101.9	100.6	104.3	105.0	100.9
		104.1	103.4	100.9	99.6	104.3	109.2	102.7
		101.7	104.0	100.7	99.1	105.1	105.7	102.3
		103.6	102.6	99.4	99.3	104.2	103.7	102.4
		99.7	104.5					
		101.0	100.0					
		104.4	101.8					
		100.8	103.3					
Average	101.5	102.1	103.5	102.3	101.0	104.2	106.6	102.5
Std.deviation	0.4	1.4	1.2	1.2	1.4	2.4	2.0	1.4

No friction conditions

	Square				Round			
Panel no.	3	1	13	5	16	2	4	14
Measured over the yield lines	102.7	102.5	102.1	103.2	101.3	101.2	101.6	103.4
	102.6	103.4	102.8	103.3	101.7	102.9	102.4	103.2
	101.7	102.4	102.1	102.6	101.4	104.7	102.6	101.9
	100.9	103.6	103.0	103.8	101.4	101.6	102.4	102.5
	102.9	102.4	101.3	102.6	100.8	104.1	100.6	103.0
	102.7	103.6	102.0	103.9	99.7	103.9	100.1	102.7
	102.8	101.6	102.4	102.3	101.3	104.5	99.8	103.0
	102.8	103.2	102.9	103.7	101.1	102.9	101.5	103.1
	101.6	103.5	101.3	102.6	101.7	102.4	101.2	103.1
	101.8	101.8	101.9	101.3	101.4	102.4	101.6	102.8
	102.7	103.0	101.8	102.2	101.4	101.1	100.7	103.4
	103.1	103.2	102.8	104.3	101.2	102.5	101.7	103.4
	102.4	103.1	103.1	103.3	101.0	103.3	100.9	102.9
	101.3	102.1	103.2	104.2	101.2	102.7	99.4	103.4
	102.5	103.2	103.0	102.0	101.7	101.8	100.1	102.7
	103.1	103.7	102.4	103.4	101.7	100.9	99.4	103.0
Average	102.4	102.9	102.4	103.0	101.3	102.7	101.0	103.0
Std.deviation	0.7	0.6	0.6	0.8	0.5	1.2	1.0	0.4

APPENDIX 5 Various results from the panel tests

Square panels, standard conditions

Sample identification:	S7	S9	S11	S15	Average	Std.dev.	COV
Averege panel thickness (mm) =	103.5	102.1	102.3	101.5	102.4	0.8	0.8 %
Correction factor (k = 100 mm/thickness) =	0.966	0.979	0.978	0.985	0.98		
Modified displacement (Δk= 25 x k) =	24.2	24.5	24.4	24.6	24.4		
(measured) EAC at 25 mm =	1123.7	1304.9	964.8	1390.6	1201.0	182.1	15.2 %
Corrected EAC [(EAC x k) at Δk] =	**1062.7**	**1261.7**	**949.2**	**1358.7**	**1158.1**	**185.9**	**16.1 %**
Maximum load (kN) =	73.9	82.8	67.7	85.2	77.4	8.1	10.4 %
Residual load at Δk (kN) =	28.6	32.7	24.9	31.5	29.4	3.5	11.8 %

Round panels, standard conditions

Sample identification:	R6	R8	R10	R12	Average	Std.dev.	COV
Averege panel thickness (mm) =	101.0	104.2	102.5	106.6	103.6	2.4	2.3 %
Correction factor (k = 100 mm/thickness) =	0.990	0.960	0.976	0.938	0.97		
Modified displacement (Δk= 25 x k) =	24.8	24.0	24.4	23.5	24.1		
(measured) EAC at 25 mm =	1159.8	1277.2	1134.9	1301.4	1218.3	83.2	6.8 %
Corrected EAC [(EAC x k) at Δk] =	**1141.9**	**1202.2**	**1092.4**	**1174.0**	**1152.6**	**47.1**	**4.1 %**
Maximum load (kN) =	80.2	91.0	72.3	89.0	83.1	8.6	10.3 %
Residual load at Δk (kN) =	26.3	24.8	25.1	33.2	27.4	3.9	14.4 %

Relation Square / Round (measured) = 0.986
Relation Square / Round (corrected) = 1.005

Square panels, no friction conditions

Sample identification:	S1	S3	S5	S13	Average	Std.dev.	COV
Averege panel thickness (mm) =	102.9	102.4	103.0	102.4	102.7	0.3	0.3 %
Correction factor (k = 100 mm/thickness) =	0.972	0.977	0.971	0.977	0.97		
Modified displacement (Δk= 25 x k) =	24.3	24.4	24.3	24.4	24.3		
(measured) EAC at 25 mm =	833.6	851.4	767.8	727.3	795.0	57.7	7.3 %
Corrected EAC [(EAC x k) at Δk] =	**799.0**	**821.3**	**736.5**	**701.1**	**764.5**	**55.4**	**7.3 %**
Maximum load (kN) =	66.4	64.1	70.8	65.4	66.7	2.9	4.4 %
Residual load at Δk (kN) =	16.5	17.9	12.8	16.4	15.9	2.2	13.6 %

Round panels, no friction conditions

Sample identification:	Ri2	Ri4	R14	R16	Average	Std.dev.	COV
Averege panel thickness (mm) =	102.7	101.0	103.0	101.3	102.0	1.0	1.0 %
Correction factor (k = 100 mm/thickness) =	0.974	0.990	0.971	0.987	0.98		
Modified displacement (Δk= 25 x k) =	24.3	24.8	24.3	24.7	24.5		
(measured) EAC at 25 mm =	875.3	654.3	749.0	712.3	747.7	93.5	12.5 %
Corrected EAC [(EAC x k) at Δk] =	**841.4**	**644.5**	**716.8**	**699.2**	**725.5**	**83.2**	**11.5 %**
Maximum load (kN) =	76.5	64.7	71.5	66.5	69.8	5.3	7.6 %
Residual load at Δk (kN) =	17.2	13.6	14.9	12.5	14.6	2.0	13.8 %

Relation Square / Round (measured) = 1.063
Relation Square / Round (corrected) = 1.054

APPENDIX 6 Measured load-deflection data

Round panels (standard conditions)	4 pages
Round panels (no friction conditions)	4 pages
Square panels (standard conditions)	4 pages
Square panels (no friction conditions	4 pages

<u>Channels</u>

"Displ."	= Vertical displacement of the load cell
"Deform. 2"	= Same as "Deform. 2 M"
"Deform. 2A"	= Displacement transducer 1 under the panel
"Deform. 2B"	= Displacement transducer 2 under the panel
"Deform. 2 M"	= Average of "Deform. 2A" and "-2B". Used for load-cell control.
"Force"	= Load-cell force

Statens vegvesen

Norwegian Public Roads Administration

Norwegian Public Roads Administration
Directorate of Public Roads
P.O.Box 8142 Dep
N-0033 Oslo
Telephone +47 915 02030
E-mail: publvd@vegvesen.no

ISSN 1504-5005